



UNIVERSITÀ
DEGLI STUDI
FIRENZE

DOTTORATO DI RICERCA IN NEUROSCIENZE E
PSICOLOGIA CLINICA
Indirizzo in Neuroscienze

CICLO XXVI

COORDINATORE Prof. Renato Corradetti

Leptomeningeal and parenchymal MS lesions evaluated by MRI at
different magnetic fields.

Settore Scientifico Disciplinare MED/26

Dottoranda

Dott.ssa Luisa Vuolo

Tutor

Prof. Massacesi Luca

Coordinatore

Prof. Corradetti Renato

Anni 2010/2014

| | |
|---|-----------|
| INTRODUCTION TO MULTIPLE SCLEROSIS..... | 4 |
| CORTICAL INVOLVEMENT..... | 7 |
| IMAGING OF MULTIPLE SCLEROSIS..... | 9 |
| CONVENTIONAL MRI | 9 |
| ULTRAHIGH-FIELD MRI | 12 |
| PART I: LEPTOMENINGEAL INFLAMMATION IN MULTIPLE SCLEROSIS | 15 |
| LEPTOMENINGES ANATOMY..... | 15 |
| LEPTOMENINGEAL INFLAMMATION IN MS | 15 |
| LEPTOMENINGEAL ENHANCEMENT | 17 |
| METHODS | 20 |
| DATA AT 3T (NIH)..... | 20 |
| PATHOLOGICAL DATA..... | 22 |
| DATA AT 1.5T..... | 25 |
| DATA AT 7 T | 26 |
| AUTOLOGOUS HEMATOPOIETIC STEM CELL TRANSPLANTATION | 28 |
| RESULTS | 30 |
| CLINICAL DATA AT 3T (NIH)..... | 30 |
| PATHOLOGICAL DATA..... | 36 |
| CLINICAL DATA AT 1.5 T | 37 |
| DATA AT 7T | 39 |
| LEPTOMENINGEAL ENHANCEMENT IN AUTOLOGOUS HEMATOPOIETIC STEM CELL TRANSPLANTATION | 40 |
| DISCUSSION..... | 42 |
| PART II: PERI-VENULAR DISTRIBUTION OF MULTIPLE SCLEROSIS LESIONS..... | 48 |

| | |
|--|-----------|
| TECHNIQUES TO IMAGE VEINS | 48 |
| PREVIOUS WORKS..... | 50 |
| AIMS OF THIS STUDY | 52 |
| METHODS | 53 |
| FLAIR* AT 7T VERSUS FLAIR* AT 3T | 53 |
| STUDY AT 1.5T | 57 |
| RESULTS | 60 |
| COMPARISON OF FLAIR* AT 3T AND 7T..... | 60 |
| RESULTS AT 1.5 T..... | 61 |
| DISCUSSION..... | 62 |
| CONCLUSIONS..... | 64 |
| REFERENCES | 66 |

Introduction to Multiple Sclerosis

Multiple sclerosis (MS) is a chronic disease of the central nervous system (CNS) with a usual onset in young adulthood, often leading to severe disability.

Most people are diagnosed between the ages of 20 and 50, although MS can occur in young children and significantly older adults.

Genetic factors are playing a significant role in determining who develops MS, as proved from the higher incidence in first-degree relatives of a person with MS, such as children or siblings. The risk of non-identical twins rises to approximately 2.5-5%. Homozygotes twins have a 25% chance of developing the disease. This means that genetic factors are relevant but also environmental factors are called out.

MS occurs in most ethnic groups, including African-Americans, Asians and Hispanics/Latinos, but is more common in Caucasians of northern European ancestry.

In general, MS is more common in areas farthest from the equator ¹. Migration from one geographic area to another seems to alter a person's risk of developing MS. Studies indicate that immigrants and their descendants tend to take on the risk level of the area to which they move.

MS is at least two to three times more common in women than in men, suggesting that hormones may also play a significant role in determining susceptibility to MS. Moreover recent studies have suggested that the female to male ratio may be as high as three or four to one ².

Potential environmental modifiable factors involved in multiple MS include low adherence to treatment, smoking, obesity, low levels of liposoluble vitamins A and D, high consumption of salt, and a sedentary lifestyle, infection with Epstein-Barr Virus. Chronic tobacco use, obesity, sedentary and insufficient levels of these vitamins all contribute to maintenance of a pro inflammatory state ³.

Typically, four distinct phenotypes have been described on the basis of the onset and progression of disease ⁴. These are relapsing-remitting (RR-MS), primary progressive (PP-MS), secondary progressive and progressive relapsing MS (SP-MS)⁴. The course of disease is very individual and variable. The cause of this heterogeneity is unknown. While some patients have a very aggressive course, others run a very mild course, none as benign MS ⁵, wherein patients do not enter the progressive form of disease.

The onset of disease is seen to be relapsing remitting in about 85% patients ⁴. *An episode of acute or subacute new neurological deficit or worsening of old symptoms, which lasts for a minimum of 24 hours*, is defined as a relapse. Symptoms evolved over days and recovery can take up to many weeks. The frequency of relapses is very variable.

In the early years of disease, the incidence of a relapse is estimated to be 1.1 times/year and this decreases with increasing duration of disease and advance to progressive disease ⁶. Pathologically relapses represent focal inflammation and demyelination in the central nervous system white matter.

When the recovery after a relapse is incomplete and there is a gradual and increasing accumulation of deficit and disability, the disease is said to enter a secondary

progressive phase. About 60% patients progress to SPMS in about 10-15 years after the onset of disease ⁶.

PPMS, on the other hand, have a progressive course from the onset to disease. This phenotype is rare and affect about the 15% of patients. About 25% of patients initially diagnosed to have PPMS, are seen to have superimposed relapses together with the progressive phase of disease and are referred to as progressive relapsing MS.

Clinical presentation can be most oddly assorted, including optic neuritis, motor and sensory deficit, ataxia, fatigue, and cognitive impairment. The disease course similarly varies to a large extent between patients.

The diagnosis of multiple sclerosis is based on demonstrating evidence of inflammatory-demyelinating injury within the central nervous system that is disseminated in both time and space.

Dissemination in time means that there must have been at least two discrete episodes of inflammatory disease activity separated by at least 1 month. Since MS is considered for definition a recurrent disease, the purpose of this requirement is to exclude all monophasic illnesses, pathologically different from MS. Nowadays, dissemination in time can be established also by MRI activity ⁷.

Dissemination in space requires that the inflammatory process occur in at least two different areas of the central nervous system.

As the dissemination in time, also the dissemination in space can be established using para-clinical evidence, primarily MRI, in addition to the clinical findings.

Cortical involvement

Although historically considered a white matter disease, there are several evidences that multiple sclerosis involves also cortex and gray matter.

This feature has been disregarded in the past years for several reasons: myelin density within the cortex is very low, mostly confined to the subpial sheet and, thus, its involvement can be lost, using conventional myelin stains; moreover cortical MR imaging is limited by several limitations (see below).

Immunohistochemical techniques are superior to classical myelin histochemical staining methods (luxol fast blue). In particular the use of antibodies specific to major myelin proteins is superior to antibodies against minor myelin proteins (PLP) was really effective in detecting cortical demyelination ⁸.

Cortical involvement is widespread and interests all the phase of the disease ⁹. The presence of cortical lesion can help in the differential diagnosis with other diseases, such as NMO ¹⁰ and migraine ¹¹.

The classification based on the location of the cortical demyelinated lesions with respect to the layers of the cortex ¹². Four types of lesions have been described from autoptic pathological studies. Type I lesions are also called *leukocortical* and involve the deeper layers of the grey matter and the subadjacent white matter at the grey/white matter junction with sparing of the superficial layers of the cortex. Type II lesions, or *intracortical* lesions, are small demyelinated lesions centered on blood vessels and included in the cortex, sparing superficial cortex and the white matter. Type III lesions extend from the pial surface into the cortex, most often reaching the cortical layers 3 or 4. Type IV lesions extend to the entire width of the cortex without entering the subcortical

white matter. Type III and IV interest the subpial area of the cortex. In particular, Type III, also note as subpial lesions, are the main factor of cortical myelin loss¹³.

These are mainly present in the sulcal folds, where the CFS is stuck, particularly in the insula, cingulate, frontal and temporal cortices, the hippocampus and the cerebellum¹⁴.

The pathogenesis of these lesions is thought to be related to meningeal inflammation¹³.

Imaging of Multiple Sclerosis

Conventional MRI

MR imaging contributes to the most recent diagnostic criteria ⁷. Nevertheless, MR is mandatory in patients' follow-up ¹⁵.

Focal white matter lesions in the brain can be depicted with T2-weighted and fluid-attenuated inversion recovery (FLAIR) images ¹⁶. MRI is very sensitive in detecting foci of demyelination but its specificity is completely insufficient. Lesions represent a combination of inflammation, demyelination, axonal loss, and gliosis.

Locations considered characteristic for MS are the periventricular and juxta cortical areas, the posterior fossa, and the spinal cord ¹⁶.

Multiple sclerosis lesions develop around a central vein. This feature is well known from the histopathology but its detection in vivo is an attractive opportunity since it could help in the differential diagnosis. This will be discussed below.

In general, the correlation between MRI measures and clinical outcomes, although positive, was found to be weak ¹⁷ but a large meta-analysis ¹⁸ of over 6500 RRMS patients in 23 randomized double-blind placebo-controlled trials showed that although the clinic-radiological paradox may still hold true in an individual patient, in large groups of patients, the treatment effect on MRI may be used to reliably predict the treatment effect on clinical course. In another meta-analysis, the same authors demonstrated a significant correlation between the effect of treatment on relapse rate and Expanded Disability Status Scale (EDSS) worsening, as well as a slightly less robust but statistically significant correlation between MRI outcomes and EDSS worsening ¹⁹.

The appearance of new lesions is marked by blood-brain barrier leakage and

characterized by lesion enhancement on postgadolinium T1-weighted images. This is considered to be a measure of disease activity. Usually, after the onset the lesion is enhancing for 3-4 weeks²⁰.

Different patterns of enhancement have been identified using dynamic contrast-enhanced (DCE) MRI²¹. Initially the enhancement appears to be centrifuge; in a latter stage the enhancement became centripetal. This concept replaces the previous idea that the enhancing ring-like lesions were more aggressive than the nodular-like one²².

Several studies reported alteration previous to the lesion appearance both in animal models²³ than in human²⁴.

A subset of T2 lesions appears dark on T1-weighted images. These T1-hypointense lesions, or T1 black holes, defined as lesion less intense than the surrounding white matter but more than cerebrospinal fluid. However, a high degree of variability is limiting the use of this feature in clinical and research settings.

Nevertheless the damage spreads beyond the lesions. More advanced quantitative MR imaging techniques such as diffusion-weighted imaging (DWI) diffusion tensor imaging (DTI), magnetic transfer imaging MTR²⁵ and spectroscopy MR document several alterations also in the *normal appearing* white matter and gray matter. These changes are widespread, interesting the overall brain; nevertheless sites typically evolved (periventricular area) present a more severe damage²⁶.

The widespread damage is documented also by SNC volume loss. Brain²⁷ and cord²⁸ atrophy can be measured with different techniques more or less automated. Although central nervous system (CNS) volume loss reflects a variety of pathogenic processes²⁹, it is relevant in the assessment of MS because of its relationship to clinical outcomes³⁰.

MS has been considered for a long time as a white matter disease, however cortical involvement is relevant as discussed earlier. Detection of cortical grey matter lesions has however remained limited using conventional MRI sequences^{31 32}. Factors limiting their visualization include: location, size, intrinsic properties of the lesions such as minimal inflammation, lack of a blood brain barrier disruption³³, a lesser degree of contrast between the lesion and surrounding tissue³⁴. Proximity to the CSF also causes susceptibility artifacts³⁵.

Double inversion recovery, which suppresses signal from both CSF and white matter, has greatly improved the visualization of grey matter lesions at clinically acceptable field strengths (1.5T).

MRI sequences that have been used for the study of cortical lesions include 2D Double inversion recovery (DIR), multi-slab 3D DIR³⁶, single slab isotropic 3D DIR⁷, MPRAGE³⁷, 3D FLAIR³⁸ and Flash T2³⁹. Consensus recommendations for detecting cortical grey matter lesions have recently been published⁴⁰.

Subpial demyelination is challenging to be detected using MRI even at highest field.

Spinal cord abnormalities, either focal or diffuse, are found 86% of patients with MS⁴¹. Frequently, cord lesions are focal, less commonly there are diffuse abnormalities. In the last case they are more often in differential diagnosis with transvers myelitis or optic neuro-myelitis (NMO). Different MRI sequences to detect lesions have been proposed, including STIR⁴², MPRAGE⁴³, axial GRE⁴⁴. However a consensus on a standardized protocol is missing. Cord MS lesions are strongly related to prognosis⁴⁵.

Another common site of demyelination is the optic nerve; its involvement is found in approximately 94–99% of autopsy cases ⁴¹.

Nevertheless optic nerve imaging is really challenging due to the limited dimensions and the proximity to the CSF, bone and fat. Optic neuritis diagnosis is essentially clinical but MRI can help and can give prognosis information. Sequences suppressing the fat and the CSF (FLAIR-STIR) showed a good visualization of lesions ⁴⁶. Recently, DIR has been proved to be efficient in detecting optic nerve lesions ⁴⁷

Ultrahigh-Field MRI

Imaging at ultrahigh magnetic field (>3.0 T) offers great advantages in signal-to-noise ratio, resolution and greater chemical shift dispersion and image contrast. It was demonstrated to be safe and well tolerated despite a mild and transitory vertigo. Some limitations restrict the routine use: the limited diffusion of magnets, the cost, the needing of high appropriate radiofrequency coils and a strenuous post-processing.

At present, ultra-high field is used only in research contests. It is extremely useful in understanding MS pathogenesis.

7T MRI is more sensitive than lower field in detecting white matter lesions ⁴⁸ and allows greater morphological details, in particular in the association with the vasculature ⁴⁹, similar to pathological reports.

The use of iron sensitive sequences has provided a new insight in the lesion characteristic, showing the presence of a paramagnetic ring around some acute and chronic lesions. In acute lesions, this rim could reflect the expanding inflammatory edge

and may directly correspond to inflammatory byproducts and sequelae of blood-brain barrier opening ⁵⁰.

Using ultra high field, cortical lesions detection has consistently improved thanks to the higher spatial resolution and contrast, despite the limits of inhomogeneity of B_0 and radiofrequencies with respect to lower fields. Therefore a better classification of cortical lesion is now possible ³⁸. At 7.0 T, the three major types of cortical lesions are identifiable and the proportions are virtually identical to those detected histopathologically ⁵¹.

In vivo MRS at high field also benefits from the increased ratio of signal to noise at an ultrahigh field. Additional metabolites relevant to MS, such as glutathione, glutamate, amino butyric acid, and ascorbic acid (vitamin C), are under active investigation, along with the macromolecular (background) signal.

Moreover, ex-vivo ultra-high MRI can guide histopathological studies ⁵².

Part I

Leptomeningeal inflammation in Multiple Sclerosis

Part I: Leptomeningeal inflammation in Multiple Sclerosis

Leptomeninges anatomy

The meninges are the membranes that envelop the central nervous system. They consist of three layers: the dura mater, which lies directly under the calvarium, the arachnoid mater, and the pia mater, in direct contact with the brain parenchyma, following the sulci. The dura mater is a loose collection of fibroelastic cells with interdigitating cell processes, no extracellular collagen, and significant extracellular space.

Between the two layers of the dura mater of the brain, there are large dural sinuses that drain blood and cerebral spinal fluid (CSF) from the cerebral vessels and ventricles, respectively. The arachnoid is a fibrous membrane formed by flattened, closely connected cells with no extracellular collagen. The pia mater, since follow brain circumvolutions, is the larger sheet. The pia is continuous with the meningeal coating of the vessels. As blood vessels transverse the pia mater, they gain elaborate tight junctions between the endothelial cells and are surrounded by astrocyte foot processes, forming the BBB of cerebral vessels.

The primary function of the meninges and of the cerebrospinal fluid is to protect the central nervous system. However, recently the meninges are gaining appreciation as non lymphoid sites of active immune responses⁵³.

Leptomeningeal inflammation in MS

The meninges house a wide variety of immune cells. Resident cells include macrophages, dendritic cells, mast cells, innate lymphoid cells, fibroblasts, and even stem cells,

whereas neutrophils, T cells, and B cells infiltrate during inflammation. Such diverse cellular responses likely allow for effective protection against microbes. But similar to other barrier sites, the meninges can be sites of chronic inflammation. There are several evidences, such as in meningitis, that meningeal inflammation has consequences for neurological functions.

A conspicuous spatial relationship between meningeal inflammation and gray matter lesions has been reported. Using immunohistochemistry to assess post-mortem tissue samples from patients with MS, Choi et al ⁵⁴ observed that high numbers of meningeal lymphocytes correlated with severe disease and death at a younger age. Damage to the glia limitans and subpial demyelination is most often observed in cases of MS with more severe meningeal inflammation ^{55 56}.

Moreover, in a limited number of secondary progressive multiple sclerosis (SPMS) the inflamed cerebral meninges contained structures, strikingly similar to secondary B-cell follicles ⁵⁷.

Follicles show some aspects of germinal centers, including proliferating B cells and a core network of stromal/follicular dendritic cells. The germinal centers support humoral immune responses towards infectious organisms by promoting B-cell homing, expansion, and differentiation into plasma cells that produce high-affinity antibodies. These follicles are similar to that found in other autoimmune diseases.

Patients follicle positive presented a wider cortical pathology, earlier disease onset, earlier onset of irreversible disability and death, higher degree at disability scales ⁵⁸.

However, B-cell follicles is not a late phenomenon in MS. Rather than using postmortem samples, Lucchinetti et al analyzed brain biopsies from patients with MS at initial disease

presentation and determined that meningeal inflammation occurred early in disease and preceded the appearance of classic white matter lesions in many patients¹³.

An abnormal accumulation of EBV-infected cells was found in post-mortem brain tissues from 21 of 22 patients with MS⁵⁹.

Leptomeningeal enhancement

Leptomeningeal enhancement is a marker of a damage of the Blood-CSF Barrier leakage.

It has been described in different pathologies. It can be diffuse or focal.

Here there is a list of the main pathologies in which has been described⁶⁰.

Diffuse

- leptomeningeal carcinomatosis, e.g. from carcinoma of breast or lung, melanoma, ependymoma
- haemorrhage, e.g. post-subarachnoid
- intracranial hypotension, e.g. after lumbar puncture or CSF leak
- meningitis
 - pyogenic meningitis
 - viral meningitis
 - tuberculous meningitis (can also be focal)
 - from CNS cryptococcal infection
- encephalitis
- granulomatous conditions
 - neurosarcoidosis (can also be focal)
- post-operative (late finding)

- post-traumatic (late finding)

Focal

- Leptomeningeal carcinomatosis, e.g. from carcinoma of breast or lung, melanoma
- hyperaemia: post-ictal
- infarction: subjacent acute (leptomeningeal collaterals) or subacute
- lymphoma
- meningitis (localised), e.g. tuberculous
- encephalitis
- Neurosarcoidosis
- scar, postoperative
- Vasculitis

Neurosyphilis

Leptomeningeal enhancement has been considered as a *red flag* in the diagnosis of Multiple Sclerosis ⁶¹, since it is unusual in MS and is more common in some disease miming MS.

A workshop of the European MAGNIMS (Magnetic Resonance Network in Multiple Sclerosis) was held to define a series of MRI red flags in the setting of clinically suspected multiple sclerosis. It was derived from evidence-based findings and educated guesses ⁶². The leptomeningeal enhancement was classified as a major red flag (score 29/30), since it was considered fairly definitively to a specific non-MS alternative diagnosis, like vasculitis, chronic meningitis, sarcoidosis, lymphomatosis.

Nevertheless, some reports describe leptomeningeal enhancement in MS ^{63 64}

Gadolinium contrast-enhanced, T2-weighted, fluid attenuated inversion recovery (T2-FLAIR) MRI is considered as much as ten-fold more sensitive than T1-weighted imaging for detecting low concentrations of contrast in cerebrospinal fluid ⁶⁵.

In MS, postcontrast T2-FLAIR offers outstanding detection of contrast enhancement within white matter lesions ⁶⁶, but leptomeningeal contrast enhancement in multiple sclerosis has not been investigated.

Thus, we retrospectively reviewed patients at 3T and 1.5T. We also ask to a small subset of patients with leptomeningeal enhancement to undergo to a 7T. Moreover, we reported two histopathological reports from two patients with leptomeningeal enhancement.

Methods

Data at 3T (NIH)

Inclusion criteria were the following: age \geq 18; clinical diagnosis of MS ⁷ or neurologically healthy; and availability of a 3-tesla, 3D T2-FLAIR scan performed at least ten min after intravenous injection of gadolinium-based contrast material. For participants with multiple scans obtained during the study period, all scans were reviewed and analyzed in one batch.

Imaging, laboratory, and clinical data were collected with Institutional Review Board approval and after written, informed consent.

MRI was obtained on two scanners: 114 on a GE Signa HDx scanner (General Electric Healthcare, Milwaukee, WI) and 222 on a Siemens Skyra scanner (Siemens AG, Erlangen, Germany). The body coil was used for radiofrequency transmission and the manufacturers' 8 (GE) and 32 (Siemens) channel phased-array head coils for signal reception. Postcontrast 3D T2-FLAIR images were obtained using product sequences provided by the manufacturer, denoted CUBE (GE) or SPACE (Siemens). Scans were performed at least ten min following intravenous injection of single-dose (0.1 mmol/kg) gadopentetate (Magnevist, Bayer AG, Leverkusen, Germany; 15% of cases) or gadobutrol (Gadavist, Bayer AG, Leverkusen, Germany; 85%). Postcontrast 3D T2-FLAIR images were obtained using product sequences provided by the manufacturer, denoted CUBE (GE) or SPACE (Siemens). Precontrast T2-FLAIR was available in 46% of cases.

We defined leptomeningeal enhancement as signal intensity within the subarachnoid space, substantially higher than signal of brain parenchyma and brighter on postcontrast scans than on precontrast scans, if available. High-signal regions adjacent to dural venous sinuses, basal meninges, and large subarachnoid veins were excluded a priori, as these were commonly present on precontrast scans, including in healthy individuals. Postcontrast T1-weighted images were always available and evaluated. Images were reviewed, using standard clinical image-viewing software and reformatting images in each plane. Sliding 10-mm maximum intensity projections were also evaluated in at least two planes.

A group of 37 neurologically healthy controls was evaluated over the same time frame as the MS cases. These control cases were derived from a variety of sources: 9 healthy volunteers, 19 healthy first-degree relatives of MS cases, and 9 healthy individuals asymptotically infected with human T-cell lymphotropic virus type I.

Two experienced observers (an attending neuroradiologist with ten years' experience in MS imaging and a neurologist, currently a radiology resident, with nine years' experience), who were masked to clinical and laboratory data, separately evaluated all scans for the presence of leptomeningeal enhancement. Discrepancies were adjudicated by consensus, and in cases with residual ambiguity, a third attending neuroradiologist with 17 years' experience made a final determination. When present, leptomeningeal enhancement was classified according to location (within a sulcus, overlying the brain convexity, along a dural fissure, or traversing several of these areas), shape (nodular,

linear, or plate-like), and number of foci, associated enhancement on post-contrast T1-weighted images, and presence or absence of contrast enhancing white matter lesions anywhere in the brain.

Brain structure segmentation was obtained using Lesion-TOADS and SPECTRE software, as previously describe⁶⁷. Total white matter lesion volume and brain and cortex volume (normalized to the intracranial volume) were recorded.

Statistical comparisons were made using Wilcoxon's rank-sum and Fisher's exact tests, and p-values are reported directly without adjustment for multiple comparisons.

Pathological data

Neuropathological evaluation focused on the brain of two progressive MS cases with a total of three stable foci of leptomeningeal enhancement that had been imaged repeatedly in vivo.

Here are detailed clinical and radiological stories:

Case#1: The patient was a 59-year-old Caucasian man with a disease course consistent with primary-progressive MS (PPMS) and disease duration (time from symptom onset to death) of 21 years. He reported the onset of neurological symptoms in 1992, when he developed left leg weakness with foot drop. Symptoms were minor over the next nine years but slowly progressed. In 2011, he began treatment in a clinical trial for PPMS. At his last complete neurological evaluation at our center, in 2013, the Expanded Disability Status Scale (EDSS) score was 6.5. In June 2013, the patient was hospitalized after onset of acute neurological symptoms due to multiple embolic strokes

affecting the brainstem (anterior medulla, paramedian pons) and anterior limb of the left internal capsule. The hospitalization was complicated by renal failure requiring hemodialysis, aspiration pneumonia, sepsis, and respiratory distress requiring intubation. The patient died at the beginning of July 2013, and the brain was donated for research purposes. Frequent in vivo brain and spinal cord MRI scans were obtained at 1.5 tesla, 3 tesla, and 7 tesla from 2006 through 2013. Spinal cord, infratentorial, periventricular, and juxtacortical lesions were typical of advanced MS. Cortical lesions were appreciated on the 7-tesla scan but were not clearly seen at 3 tesla. The parenchymal lesion burden was severe, and there were no new contrast-enhancing lesions in any of the available scans. The ventricles and sulci were severely prominent and noticeably increased in size over time, signifying brain atrophy. Stable, nodular contrast enhancement within a right frontal sulcus, typical of the findings reported above in the entire MS cohort, was detected in all 7 available postcontrast T2-FLAIR scans, on different 3-tesla scanners, over the final 2.5 years of follow-up.

Case#2: The patient was a 66-year-old Caucasian woman with a disease course consistent with primary-progressive MS (PPMS) and disease duration (time from symptom onset to death) of 20 years. The patient was diagnosed with MS in 2000, the disease onset was 6 years before. Her subsequent clinical course was characterized by gradually progressive worsening of sensory and motor function. In 2006, she began therapy with natalizumab. In April and May of 2013, she was noted to have decreased verbal fluency and difficulty with pronunciation during a scheduled clinic visit for her 77th dose of natalizumab. Brain MRI showed presence of numerous new non-enhancing lesions throughout both middle cerebellar peduncles and dentate nuclei. Based on clinical

deterioration and underlying changes by MRI, progressive multifocal leukoencephalopathy (PML) was considered and natalizumab treatment discontinued. In November 2013, the Expanded Disability Status Scale (EDSS) was 7.5. Frequent brain MRI scans are available at 1.5 tesla and 3 tesla field strengths from 2011 and 2013. Spinal cord, infratentorial, periventricular, juxtacortical, and cortical lesions were typical of advanced MS. The parenchymal lesion burden and atrophy was severe. In November 2013, there was confluent T2 signal abnormality in the pons extending through the middle cerebellar peduncles bilaterally, more on the right, without associated enhancement or mass effect; these findings were thought to be due to PML. Five supratentorial, focal areas of leptomeningeal contrast enhancement were detected in all 5 available postcontrast T2-FLAIR scans between 2011 and 2013 (including several scans prior to the onset of clinical symptoms attributable PML). Earlier scans had not included a postcontrast T2-FLAIR sequence. Two of those 5 foci of leptomeningeal enhancement were located in the left parietal lobe and have been histologically characterized.

Accurate registration of in vivo MRI to pathology was achieved via 7-tesla MRI of the fixed brains and subsequent gross sectioning with an individualized, MRI-designed, 3D-printed cutting box⁵². For comparison, a block of tissue in the left temporal lobe from the first patient was selected for the presence of extensive cortical pathology, as seen on postmortem MRI, but absence of in vivo leptomeningeal enhancement. Formalin-fixed, 10- μ m cryosections or paraffin sections were stained with hematoxylin and eosin (H&E) and Luxol fast blue/periodic acid Schiff (LFB-PAS) and compared with MRI.

Immunohistochemical analysis for myelin proteolipid protein, CD45, CD68, CD3 and CD20 was performed on representative slides.

Data at 1.5T

The aim of the study was to assess the reproducibility of this finding through different magnetic field and different MRI protocols.

Patients afferent to the *regional center for Multiple Sclerosis* (Tuscany-Italy) were follow up with a yearly MRI, or twice yearly if they presented clinical or radiological activity.

MRI were acquired with a standardized protocol including:

- T1-MPRAGE
- Gad injection (0.1 mmol/kg)
- T2 sag
- FLAIR axial (slice thickness =4 mm, gap =0)
- T2-ax
- T1-MPRAGE

Exams were acquired on two different machines: on a Philips Intera scanner, head coil 12ch, until February 2014; after February 2014, exams were acquired on a Philips Achieva scanner, head coil 8ch.

The FLAIR was acquired after 3 minutes of intravenous injection of single-dose (0.1 mmol/kg) gadopentetate (Magnevist, Bayer AG, Leverkusen, Germany, unknown % of cases), gadobutrol (Gadavist, Bayer AG, Leverkusen, Germany, unknown % of cases) or Gadobenic acid (Multihance, Bracco, Minneapolis, USA, unknown % of cases).

All the patients presented a clinically definite diagnosis of MS in accordance with the 2010 revised McDonald criteria ⁷.

Patients with at least one MRI from January 2013 to December 2014 were included in this retrospectively study.

For patients with multiple exams, the last MRI was evaluated. Images with movement artifact were excluded.

Images were evaluated on a dedicate console (Carestream) by an expert evaluator with 9 years of experience in MS imaging.

Criteria for leptomeningeal enhancement were the same as the 3T populations, that means a signal intensity within the subarachnoid space, substantially greater than that of brain parenchyma and brighter on postcontrast scans. Similarly, high-signal regions adjacent to dural venous sinuses, basal meninges, and large subarachnoid veins were excluded a priori. Unfortunately, precontrast FLAIR was never available, as not included in the protocol.

Images considered uncertain were evaluated again after at least a week.

Data at 7 T

A subset of patients that were found positive at 3T for the presence of at least one focus of leptomeningeal enhancement underwent to a 7 T scan (Siemens, NIH).

The aims of this study were:

- To explore the spatial location of leptomeningeal enhancement relative to blood vessels.
- To investigate if 7T is more sensitive than 3T to leptomeningeal enhancement.

- To investigate the relationship with cortical pathology

Different sequences were tested:

- T2w-FLAIR pre and post gad (gadobutrol)
- CISS
- T1w-MPRAGE
- T2*w pre and post gad (gadobutrol)
- FLAIR and MPRAGE post gadofosveset

Three-dimensional (3D) constructive interference in steady state (CISS) is a gradient-echo MRI sequence heavily T2 weighed. Thanks to this feature, it plays an important role in evaluating structures surrounded by CSF. It is mostly employed in the study of the posterior fossa where CSF surrounds the cranial nerves. We implemented a very high resolution CISS (Voxel resolution: $0.6 \times 0.6 \times 0.6 \text{ mm}^3$). We used this sequence to look for soft tissue in the site of the enhancement, taking advantage from the high quality contrast with the CSF.

The gadofosveset is a gadolinium-based contrast agent characterized by an impressive high degree of binding albumin serum. Thanks to this feature, gadofosveset is used in clinical practice for MRI angiographies. In MS, it has been used as a contrast agent and it showed a late enhancement of lesions not enhancing with other gadolinium contrast agents^{68 69}. The rationale in using this contrast agent was to evaluate the amount of the opening of the CSF-blood barrier.

Autologous hematopoietic stem cell transplantation

Autologous hematopoietic stem cell transplantation (AH SCT) following a high dose immunosuppressive treatment is a conventional therapy for patients with lymphoproliferative diseases. In autologous HSC transplantation, the immune system is partially or completely wiped out, followed by reinfusion of the patient's own hematopoietic stem cells. Given the immune system reset, it has been proposed as a therapeutic option for patients with autoimmune diseases. In Multiple Sclerosis, it is considered a valid option for patients with high inflammation activity and not responsive to approved therapies⁷⁰. Since the end of the '90, there are at least 393 registered transplantations in MS patients, according to the European BMT registry.

AH SCT has been proved to have a terrific effect in suppressing clinical and MRI-detectable inflammation⁷¹.

The effect on disease progression is less evident and only a little over half of patients is progression free on a longer follow up⁷².

Recently, a randomized trial proved the efficiency of the bone marrow transplantation against an immunosuppressive therapy (mitoxantrone) in reduction new T2 lesions⁷³.

Localized and compartmentalized inflammation in the CNS, which seems to be one of the responsible for progression of disability, is less affected by the current drugs. A more radical approach such as ASCT could theoretically suppress this inflammation in MS.

Despite literature data suggest that oligoclonal bands persist in CSF after transplantation⁷⁴ a deep immunological mutation has been described⁷⁵.

The aim of this small retrospectively study was to assess the prevalence of leptomeningeal enhancement in patients treated with AHSCT.

Inclusion criteria were: MS patients treated with AHSCT with at least one MRI according to the protocol previously described after the transplantation.

Results

Clinical data at 3T (NIH)

Data from 299 consecutive MS cases and 37 age-matched neurologically healthy controls were obtained between October 2009 and December 2013 and are included in this report.

| | <i>all MS</i> | <i>CIS</i> | <i>RRMS</i> | <i>SPMS</i> | <i>PPMS</i> | <i>Healthy</i> |
|---|---------------|----------------|--------------|----------------|--------------|----------------|
| # of participants | 299 | 10 | 171 | 44 | 74 | 37 |
| <i># female</i> | 177 (59%) | 7 (70%) | 111 (65%) | 24 (55%) | 35 (47%) | 18 (48%)* |
| <i>median age in years (IQR)</i> | 48 (18) | 49 (30) | 42 (18) | 58 (11) | 55 (12) | 42 (17)‡ |
| <i>median years since symptom onset (IQR)</i> | 8 (14) | 1 (2) | 5 (9) | 24 (14) | 10 (10) | |
| EDSS median score (25th, 75th) | 2 (1.5,6) | 1.5 (1.5,2) | 1.5 (1,2) | 6.5 (6,6.5) | 6 (3,6.5) | |
| # on disease-modifying treatment at first evaluation | 105 (35%) | 0 (0%) | 95 (56%) | 7 (16%) | 3 (4%) | |

On postcontrast T2-FLAIR MRI, the overall prevalence of leptomeningeal enhancement in the MS cohort was 74/299 (25%). Leptomeningeal enhancement was found as a single focus in 48/74 cases (65%) and multiple foci in 26/74 (35%). In sum, 109 foci were found, of which 99 (91%) were supratentorial, without predilection for a particular lobe or hemisphere. With respect to shape, 53/109 (48%) were nodular, 44/109 (40%) were linear, and 12/109 (11%) were plate-like. Most foci (61/109, 56%) were found within a single sulcus, but 8/109 (7%) traversed several sulci. Of the remainder, 21/109 (19%) were apposed to the pial surface on the cerebral convexity, and 19/109 (17%) were within a fissure. Subtle hyperintense signal was identified on postcontrast T1-weighted images in 76/109 (70%) foci; the other foci showed no enhancement relative to precontrast scans. Enhancing foci were always found in proximity to one or more vessels.

Of the enhancement-positive MS cases, 42/74 (57%, accounting for 62/109 enhancing foci) had at least one previous scan. The mean follow-up interval was 1.4 years, and the longest follow-up interval was 5.5 years. Of the 62 foci, 53 (85%) were stable in shape and size, one disappeared, and two fluctuated over time. Six new foci were appreciated in four cases.

The prevalence of leptomeningeal enhancement was 1.7-fold ($p=0.009$) higher in progressive MS (39/118 cases, 33%) than in relapsing-remitting MS (35/181, 19%). Prevalence was highest in primary-progressive MS (28/74 cases, 38%). There was no independent effect of sex. Median age ($p=0.0003$), disease duration measured as time since first symptoms attributable to MS ($p=0.0002$), and Expanded Disability Status Scale ($p=0.04$) were higher in MS cases with leptomeningeal enhancement; normalized brain volume was lower ($p=0.05$). There was no association between leptomeningeal enhancement and the presence or absence of contrast-enhancing white matter lesions, total white matter lesion volume, or disease-modifying treatment status.

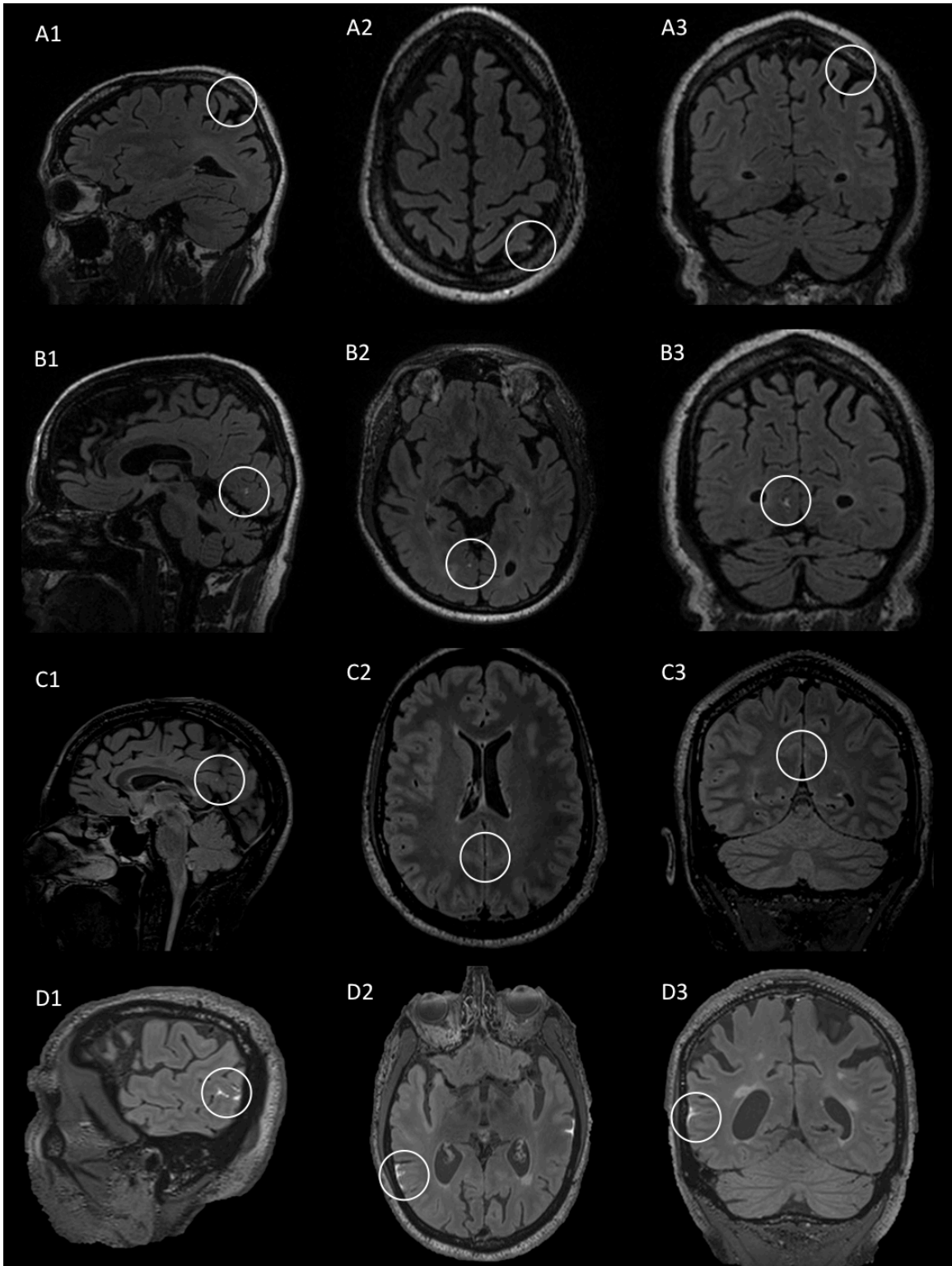
In 221/299 (74%) of MS cases, results of cerebrospinal fluid examination were available for comparison. There was no association of leptomeningeal enhancement with the cerebrospinal fluid-specific oligoclonal bands that were present in 91% of cases, or with elevated immunoglobulin-G index (cerebrospinal fluid-to-plasma ratio), white blood cells, or protein.

One of 37 (2.7%) healthy controls presented a single focus of leptomeningeal enhancement ($p=0.001$ vs. the MS cohort). In this 46-year-old healthy volunteer, a

nodular focus of leptomeningeal enhancement was seen on the post-contrast T2-FLAIR scan in the right frontal region.

Note that there was no difference in the frequency of leptomeningeal enhancement detection between MRI scanners ($p=0.49$) or between contrast agents ($p=0.71$).

Characteristics of leptomeningeal enhancement in multiple sclerosis cases ($n=299$)



Examples of leptomeningeal enhancement foci at 3 T. *Leptomeningeal enhancement was classified as apposed to the pial surface on the cerebral convexity (21/109 cases,*

19%; row A), within a sulcus (61/109, 56%; row B), along a dural fissure (19/109, 17%; row C), or traversing several of these areas (8/109, 7%; row D). The first column shows acquired images in the sagittal plane, the second column axial reformations, and the third column coronal reformations. In Row A, a nodular focus of leptomeningeal enhancement overlies the cerebral convexity in a 55-year-old man with relapsing-remitting MS (EDSS=2.5); this individual had six overall foci of leptomeningeal enhancement, the most in our cohort. In Row B, a second nodular focus from the same individual is seen within a left occipital sulcus. In Row C, a nodular focus of leptomeningeal enhancement is seen within the interhemispheric fissure in a 53-year-old male with secondary progressive MS (EDSS= 6.5). In Row D, bitemporal leptomeningeal enhancement is depicted in the axial plane in a 60-year-old man with primary-progressive MS (EDSS=6); the right-sided focus is shown in all 3 planes.

Leptomeningeal enhancement distribution and characteristics at 3T.

| Variable | Population | Leptomeningeal enhancement | | P value * |
|--|---------------|----------------------------|---------------|----------------------|
| | | Yes | No | |
| <i>time from contrast injection in min, median (IQR)</i> | 26 (11) | 26 (11) | 26 (10) | 0.55 |
| Scanner | | | | |
| # General Electric (%) | 113 (38%) | 30 (27%) | 83 (73%) | 0.58 |
| # Siemens (%) | 186 (62%) | 44 (24%) | 142 (76%) | |
| T2-FLAIR pre gad available | | | | |
| # yes | 138 (46%) | 34 (25%) | 104 (75%) | 1 |
| # no | 161 (54%) | 40 (25%) | 121 (75%) | |
| contrast type | | | | |
| # gadopentetate (%) | 50 (17%) | 12 (24%) | 38 (76%) | 1 |
| # gadobutrol (%) | 249 (83%) | 62 (25%) | 187 (75%) | |
| Sex | | | | |
| # women (%) | 177 (59%) | 43 (24%) | 134 (76%) | 0.89 |
| # men (%) | 122 (41%) | 31 (25%) | 91 (75%) | |
| <i>age in years, median (IQR)</i> | 48 (18) | 53 (16) | 46 (18) | 0.0003 |
| <i># years since symptom onset, median (IQR)</i> | 8 (14) | 11 (15) | 7 (13) | 0.0002 |
| clinical subtype | | | | |
| # MS (%) | 299 (88%) | 74 (25%) | 225 (75%) | 0.002 |
| # healthy (%) | 42 (12%) | 2 (5%) | 40 (95%) | (0.02 [†]) |
| # relapsing-remitting (%) | 181 (61%) | 35 (19%) | 146 (81%) | 0.009 |
| # progressive (%) | 118 (39%) | 39 (33%) | 79 (67%) | |
| # relapse-onset (%) | 225 (75%) | 46 (20%) | 179 (80%) | 0.005 |
| # progressive-onset (%) | 74 (25%) | 28 (38%) | 46 (62%) | |
| <i>EDSS, median (25th, 75th)</i> | 2 (1.5, 6) | 2.5 (1.5, 6.5) | 2 (1.5, 6) | 0.04 |
| disease-modifying therapy (%) (information unavailable for 1 case) | | | | |
| # treated (%) | 104 (35%) | 28 (27%) | 76 (73%) | 0.58 |
| # untreated (%) | 194 (65%) | 46 (24%) | 148 (76%) | |
| contrast-enhancing white matter lesions (information unavailable for 1 case) | | | | |
| # present (%) | 63 (21%) | 17 (27%) | 46 (73%) | 0.62 |
| # absent (%) | 235 (79%) | 56 (24%) | 179 (76%) | |
| <i>white matter lesion volume in mm³, median (IQR)</i> | 9.6 (10.7) | 10.0 (11.9) | 9.3 (10.3) | 0.56 |
| <i>normalized brain volume, median (IQR)</i> | 0.792 (0.037) | 0.786 (0.040) | 0.794 (0.035) | 0.05 |
| <i>normalized cerebral cortical volume, median (IQR)</i> | 0.361 (0.035) | 0.358 (0.031) | 0.364 (0.029) | 0.03 |
| cerebrospinal fluid-specific oligoclonal bands (information unavailable for 78 cases) | | | | |
| # present (%) | 201 (91%) | 52 (26%) | 149 (74%) | 0.79 |
| # absent (%) | 20 (9%) | 4 (20%) | 16 (80%) | |

| | | | | |
|---|-------------|-------------|-------------|------|
| cerebrospinal fluid IgG index, median (IQR) | 0.73 (0.52) | 0.74 (0.58) | 0.73 (0.52) | 0.97 |
| cerebrospinal fluid pleocytosis (white blood cells>5/mm³) (information unavailable for 57 cases) | | | | |
| # present (%) | 50 (20%) | 6 (10%) | 24 (13%) | 0.65 |
| # absent (%) | 192 (80%) | 52 (90%) | 159 (87%) | |
| cerebrospinal fluid protein (protein>45mg/dL) (information unavailable for 54 cases) | | | | |
| # elevated (%) | 73 (30%) | 19 (32%) | 54 (30%) | 0.74 |
| # normal (%) | 172 (70%) | 41 (68%) | 131 (70%) | |

* p values determined by Wilcoxon's rank sum test for continuous variables and Fisher's exact test for discrete variables.

‡ p value for relapsing-remitting MS vs. healthy.

Pathological data

Three foci of nodular leptomeningeal enhancement were consistently detected in all in vivo post contrast T2-FLAIR scans in the two progressive MS cases that later came to autopsy. The gyri flanking these sulci were affected by confluent cortical demyelination, visible as high signal intensity on the postmortem 7-tesla MRI and confirmed with myelin proteolipid protein immunohistochemistry. Diffuse leptomeningeal perivascular inflammation including T cells, B cells, and macrophages, was detected in the leptomeninges in the areas where in vivo enhancement had been present. A sulcus in the contralateral temporal lobe from the first case, which had no in vivo leptomeningeal enhancement but was identified on postmortem MRI (and later confirmed pathologically) to be associated with flanking subpial cortical lesions, showed no perivascular clusters of inflammatory cells

Clinical data at 1.5 T

From January 2013 and December 2014, 260 consecutive MS cases were obtained.

Relapsing patients were widely predominant: 212/260 (81%).

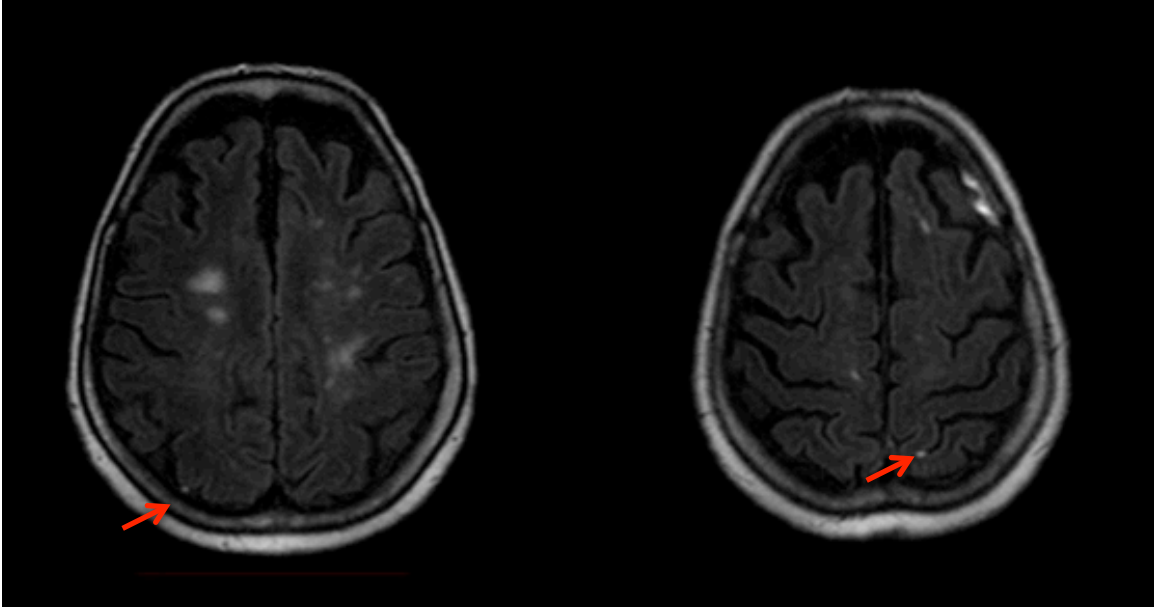
| | <i>all MS</i> | <i>CIS</i> | <i>RRMS</i> | <i>SPMS</i> | <i>PPMS</i> |
|---|---------------|------------|--------------|--------------|-------------|
| # of participants | 260 | 0 | 212 | 48 | 0 |
| <i># female</i> | 190 | - | | | - |
| <i>median age in years (IQR)</i> | 45 (15) | - | 42.7 (15) | 48.9 (15) | - |
| <i>median years since symptom onset (IQR)</i> | 14.6 (11) | - | 13.3 (10) | 19.5 (12) | - |
| EDSS <i>median score</i> (25 th , 75 th) | 1.5 (1,3) | - | 1 (1,2) | 5.5 (4,6.5) | - |

The overall prevalence of leptomeningeal foci was 27/260 (13%).

The prevalence was higher in patients with progressive course: 9/47 (17%). In the relapsing patients the prevalence was 18/212 (9%).

Age was higher in patients with leptomeningeal enhancement (p=0.03). No correlation with disease duration and EDSS was found.

| | <i>Leptomeningeal enhancement</i> | | <i>TOT</i> | |
|-------------------------|-----------------------------------|-----------|--------------|--------|
| | <i>yes</i> | <i>no</i> | | |
| # all MS | 27 (11%) | 233 (89%) | 260 | |
| <i># Progressive</i> | 9 (17%) | 39 (83%) | 47 | |
| <i># Relapsing</i> | 18 (9%) | 194 (91%) | 212 | |
| <i>Age</i> | 48 (11) | 43.5 (15) | 45 (15) | p<0.05 |
| <i>Disease duration</i> | 18 (15) | 14 (11) | 14.6 (11) | p=0.3 |
| <i>EDSS</i> | 2 (4,1) | 1.5 (3,1) | 1.5 (1,3) | p=0.4 |



Example of leptomeningeal enhancement at 1.5T. *Two foci of leptomeningeal enhancement (arrows) in a 62-year-old woman with a secondary progressive multiple sclerosis (EDSS=6, disease duration= 18 years).*

Data at 7T

15 patients (11 RRMS, 2 PPMS, 2 SPMS) with at least one focus of leptomeningeal enhancement were acquired. Median EDSS was 2 and mean age: 44 y (± 12).

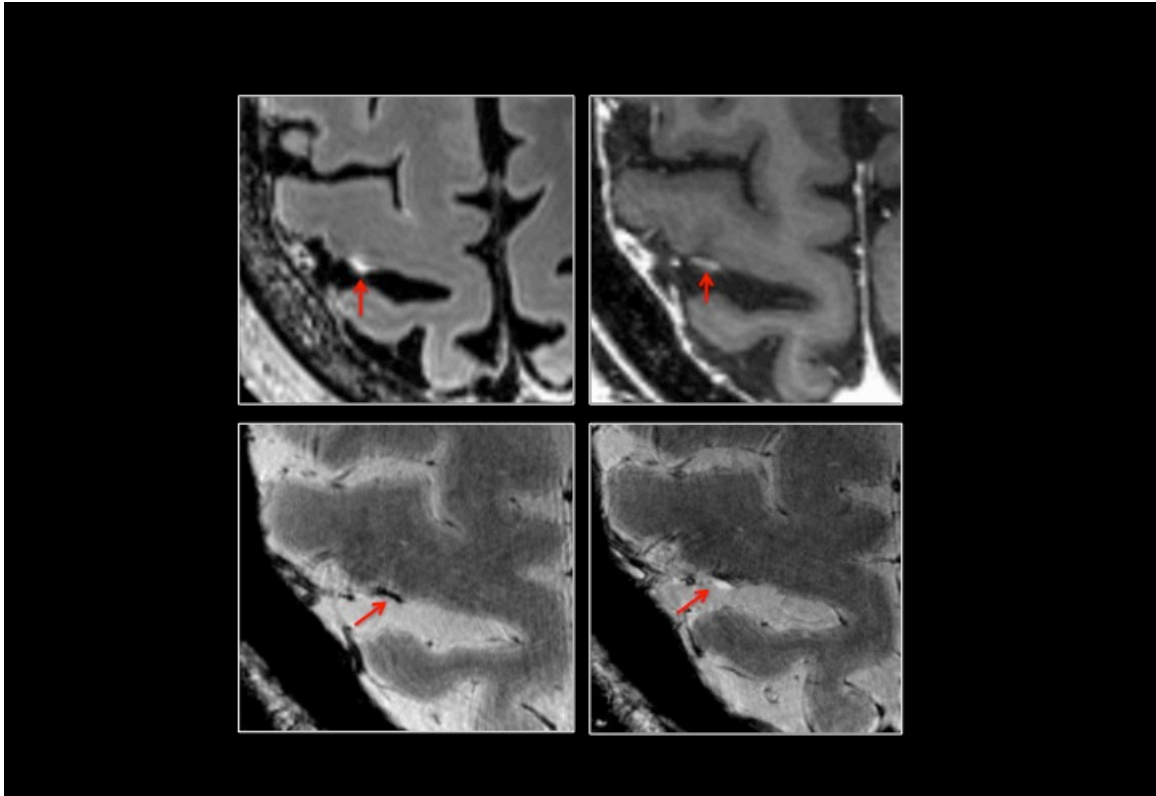
The foci of leptomeningeal enhancement depicted on the 3T FLAIR were stable as extension and location.

Sensitivity of 7T for meningeal enhancement was similar to 3T, since no new focus was found.

High resolution imaging at 7T showed focal accumulation of gad in the subarachnoid space due to an abnormal blood-CSF barrier. Gadolinium contrast was appreciable on different sequences, beyond the FLAIR. The T2* GRE showed a clearly association with one or more meningeal vessels.

Despite the high resolution, no clear associated soft tissue abnormality was identified.

In 6 of 15 patients, we found cortical lesions subjacent to foci of leptomeningeal enhancement.



Leptomeningeal enhancement at 7T. High-resolution 7-tesla MRI from a 51-year-old woman with primary-progressive MS (EDSS=6.5) shows a focus of leptomeningeal enhancement. In the first row, a FLAR post gad and a T1 post gad. In the second row a T2* respectively pre and post gad.

Leptomeningeal enhancement in autologous hematopoietic stem cell transplantation

Twenty-six patients treated with AHSCT and with one MRI according to the protocol were included. Mean age was 40 years (± 12). Median EDSS was 6 (range 4-7.5). Mean time after the AHSCT was 6 years (± 4).

| | AHSCT | Total population | |
|---------------|-----------------|------------------|---------|
| #cases | 26 | 260 | |
| Mean age (SD) | 40 (± 12) | 45 (± 10) | p=0.12* |

| | | | |
|-------------|---|-----|---------|
| Median EDSS | 6 | 1.5 | P<0.05* |
|-------------|---|-----|---------|

*Wilcoxon's test

Patients were matched for age but the EDSS was significantly higher in patients treated with AHSCT.

Of the 26 patients, no foci of leptomenigeal enhancement were found.

The frequency of leptomenigeal enhancement in patients treated with AHSCT was compared with the total population (Fisher's exact test).

No significantly difference was found.

Discussion

Inflammation in the leptomeningeal compartment has been widely described in MS from pathological reports as clustered inflammatory cells in the subarachnoid space. In this study, we proposed the first in vivo marker.

We retrospectively reviewed T2-FLAIR acquired post gadolinium contrast agents from almost 600 patients (299 at 3T and 260 at 1.5T) and we reported that small foci of leptomeningeal enhancement are a common finding in multiple sclerosis, despite leptomeningeal enhancement has been considered for a long time as a red flag in MS diagnosis⁶².

Interestingly, we retrospectively reviewed routine MRI exams. Leptomeningeal enhancement has never been mentioned in the reports, thus the finding was really subtle and required a trained observer.

The prevalence was of 25 % of the overall MS population at 3T and 12% of the overall population at 1.5T.

The main reasons for the lower prevalence at 1.5T were essential technical issues: the delay after gad injection was shorter (3 minutes) and the FLAIR wasn't a volumetric sequence.

However, even the prevalence on 3T was lower of that found in pathological reports⁵⁷. It is impossible to estimate leptomeningeal enhancement sensitivity and the relationship between the inflammation and the enhancement. It might be possible that we are only able to detect the 'peak of the iceberg' of the inflammation. Nevertheless, at present, this is the only marker available.

On regard of the specificity, this study focused on MS, so we cannot comment directly on the prevalence of leptomeningeal enhancement on T2-FLAIR in other inflammatory central nervous system disorders. Nevertheless, we reported one focus of leptomeningeal inflammation in a healthy volunteer. However, we do not expect that this finding will be diagnostically specific for MS. At the same time, our data indicate that focal leptomeningeal enhancement should not exclude the diagnosis of MS, as some prior reports have advised.

We found a relative preponderance in the progressive group relative to the relapsing-remitting. Despite the difference in prevalence, the ratio between relapsing and progressive patients was similar in the two retrospectively studies. The higher prevalence in progressive patients is consistent with the pathological studies⁵⁷.

However, leptomeningeal enhancement is not exclusively a late phenomenon. Indeed, the presence of leptomeningeal inflammation in early MS has been demonstrated in biopsy studies¹³

When we observed foci longitudinally, we appreciated their appearance but never their disappearance. This finding suggested that the leptomeningeal foci are going to accumulate, independently from disease modifying therapies. This data can explain the direct relationship between prevalence, patients' age and disease duration, among 3T data. 1.5T data did not confirm the relationship with the disease duration, suggesting that age is the strongest predictor of leptomeningeal enhancement.

Pathological data from two patients support our hypothesis. We found a diffuse leptomeningeal perivascular inflammation including T cells, B cells, and macrophages, in

the areas where in vivo enhancement had been present. A control sulcus didn't present such infiltrate.

Moreover the same sulci presented an extended cortical demyelination. However we were not able to explore this relationship in vivo, since the visualization of the subpial demyelination in vivo is really arduous. 7T data showed a cortical involvement in more than half patients, but just a limited number of patients underwent to a 7T scan. Furthermore, the relationship between leptomeningeal enhancement and cortical pathology was not univocal since we found cortical lesions also in sulci far from the leptomeningeal enhancement.

Indeed, 7T data confirmed pathological findings. High-resolution images showed that the enhancement foci were an abnormal accumulation of gadolinium in the subarachnoid space. Probably the sustained inflammation produces an abnormal opening of the CSF-blood barrier, determining a leaking of gadolinium.

Ultra-high field MRI didn't increase the sensitivity in detecting leptomeningeal foci; on the other hand we can't compare 1.5T and 3T sensitivities since the delay after the gad injection was different (3 minutes versus more than 10 minutes).

On regard of the therapies effect, we didn't analyze single drugs action. However the use of disease modifying drugs, didn't impact the presence of leptomeningeal enhancement. Future prospective studies will be required to examine specific effects of specific therapies, including corticosteroids, on the prevalence and incidence of leptomeningeal enhancement. In a single relapsing-remitting MS case we observed transient resolution of focal leptomeningeal enhancement following intravenous infusion of 1 g of methylprednisolone for five days.

Even if we didn't explore the effect of single drugs, we reported preliminary data from patients treated with AHSCT. None of the 26 patients presented leptomeningeal enhancement.

This study presents several limitations: first, the small number of patients treated with AHSCT; moreover we don't know if these patients presented leptomeningeal enhancement before the treatment and, nevertheless time between the MRI and the transplantation was different.

However, even if we didn't find any significant difference, probably due to the small number, these data are suggesting that an aggressive immune depressive therapy can act also on meningeal inflammation.

Our control group presented some limitation: first of all the number was small; moreover some of these patients presented a predisposition to neurological diseases (HTLV infection, first grade relatives of MS patients). Some of them presented aspecific white matter lesions, like the only healthy volunteer positive to leptomeningeal enhancement.

In summary, leptomeningeal enhancement is a reproducible marker over different magnetic fields and protocols. Pathological data and ultra-high field MRI confirm our hypothesis.

Further work should aim to improve sensitivity of leptomeningeal contrast enhancement, to describe in more detail the natural history of that enhancement, and to assess in prospective studies the extent to which it is affected by specific treatments.

Nonetheless, the impact on clinical practice could be impressive. Patients with leptomeningeal inflammation could be selected to a more aggressive therapy. Moreover

the effect of current therapy could be explored monitoring patients with leptomenigeal inflammation.

Targeting the cells and molecules mediating inflammatory responses within the meninges offers promising therapies for MS that are free from the constraints imposed by the BBB.

Part II

Perivenular distribution of Multiple Sclerosis lesions.

Part II: Peri-venular distribution of Multiple Sclerosis lesions.

Multiple sclerosis lesions develop around a central vein. This feature is well known from histopathology. Chorcot first described this feature in 1968⁷⁶. Later, Dawson, describe the shape of the lesions perpendicular to the ventricle (Dawson's fingers), following the veins⁷⁷.

The vein constitutes the substrate for the development of the lesions⁷⁸, in line with the widely held hypothesis that the formation of an MS lesion depends on the entry of inflammatory cells from the systemic circulation into the brain parenchyma.

Techniques to image veins

Common techniques used to image the venous system such as *Time of flight* (TOF) doesn't have enough spatial resolution to visualize small parenchymal veins, since their diameter is in the order of 100 micron.

Other techniques essentially based on the T2* effect are used.

T2* relaxation refers to decay of transverse magnetization caused by a combination of spin-spin relaxation and magnetic field inhomogeneity. T2* relaxation is seen only with gradient-echo (GRE) imaging because transverse relaxation caused by magnetic field inhomogeneities is eliminated by the 180° pulse at spin-echo imaging.

Owing to the paramagnetic effect of the Deoxyhemoglobin, venous blood, full of this paramagnet substance, perturb the local magnetic field. Thus, on a T2* weighted sequence, vein will appear hypointense relative to the surrounding tissue.

Susceptibility Weighted Imaging (SWI) is a relatively new technique based on the on the same effect of the T2*. However SWI is not simply a T2*-weighted imaging approach and consists of using both magnitude and phase information. Usually, phase information are discharged and not used. In SWI, phase information is used to enhance the endogenous contrast. The phase shift present in a GRE image represents an average magnetic field of protons in a voxel, which depends on the local susceptibility of the tissues. Paramagnetic substances, such as deoxyhemoglobin, hemosiderin, and ferritin, increase the magnetic field, resulting in a positive phase relative to the surrounding parenchyma. For a left-handed (or right-handed) system, the phase is positive (or negative) when the spins process clockwise. Diamagnetic substances, such as calcium, cause a negative phase shift. Phase images are sensitive to changes in the magnetic field caused by different components in tissues, such as deoxyhemoglobin, hematoma, or calcification, and can be used for differentiating the susceptibility differences among tissues. Phase itself can be an excellent source of contrast, with or without T2* effects ⁷⁹. A phase “mask” can be created which, when multiplied with the magnitude phase image improves the contrast of veins without dramatically changing other contrast.

The contrast of lesions may not be optimal on T2* or SWI images compared to FLAIR, that is the clinical standard for lesion detection. Thus, Grabner ⁸⁰ used a fused approach and created a new image from a FLAIR at 3 T and a phase mask at 7T. He combined the efficiency of the FLAIR to visualize the lesions and the efficiency of the T2* to visualize the veins. But this approach needs to different acquisitions on two different magnetic field. Thus, Sati ⁸¹ applied the same concept at a 3T MRI. The image resultant was called

FLAIR*. The technique consists in multiply the SWI phase mask with a co-registered FLAIR. The administration of exogenous contrast agents such as gadolinium increases the phase effect around blood vessels, improving their visibility.

Recently, the FLAIR* has been applied to a 7 T MRI ⁸².

Previous works

In 2000, Tan et al firstly used MRI to demonstrate that MS lesions are venocentric ⁸³

Impressively, this study remains the only attempt at 1.5 T. Among 95 MS lesions identified, the venograms showed a vein running centrally in all but one subcortical lesion. The orientation and form of the MS lesions corresponded well with the course of this vein, confirming their perivenous origin.

Subsequent studies in 2008 used higher-field-strength magnets, improving the vein visualization and achieving results comparable with the pathology ^{84 85}.

Tallantyre ⁸⁶ compared the 7T T2* to the 3 T T2* in detecting intralésionnal vessels, demonstrating the superiority of the 7T in detecting this feature. A central vessel was identified in 45% of visible lesions using 3T T2* and 87% of visible lesions using 7T T2* (P < 0.0001).

Despite these different percentages of lesions with vein showed by different techniques, the association between MS lesions and vein appear to be strong.

However the specificity of this feature for MS and thus the possibility to use it in the differential diagnosis is still unexplored. Few studies investigated this feature in other diseases.

Lummel ⁸⁷ et al studied a population of patient 15 patients with MS and 15 patients with

microangiopathic white matter lesions. They didn't find any significant difference between groups with regard to the percentage of lesions with central vein, suggesting that central vein within a WML should not be considered as a specific finding for MS.

Controversy, another study showed a significantly difference in microangiopathic lesions⁸⁸, suggesting a role of T2* in the differential diagnosis.

In Susac Syndrome, at 7 T the percentage of lesions with vein was lower than in MS patients⁸⁹.

Ten patients with a neuromyelitis optic (NMO) - spectrum disorder were evaluated for the presence of a vein inside the lesions, using a T2* weighted sequence at 7T. The percentage of lesions with the vein was significant lower in patients with NMO spectrum disorder with respect to patients with MS⁹⁰.

But although other diseases showed a low incidence of perivenular lesions, the utility of in the diagnosis of MS is still debatable. Only 2 prospective studies explored the efficiency to discriminate between MS and other conditions with white matter lesions and to evaluate the prediction to convert to clinically defined MS.

In a 3T SWI study, Kau et al. studied 14 patients with white matter lesions. Later 5 patients fulfilled MS diagnostic criteria, 9 received another diagnosis. All the lesions with a vein, but one, were MS lesions⁹¹. In this study just lesions larger than 5 mm were considered.

Mistry et al⁹² followed 29 patients with suspect MS. T2*-weighted 7-T MRI was acquired at baseline and analyzed blinded to clinical data. Twenty-two of 29 patients received a clinical diagnosis. All the 13 patients diagnosed as MS presented a vein in the majority of the lesions. Nine patients diagnosed as other disease presented a vein in a

minority of lesions. They concluded that the T2*-weighted 7-T MRI had 100% positive and negative predictive value for the diagnosis of MS

Aims of this study

- Compare the efficiency of the FLAIR* at 3T and the FLAIR* at 7T
- Implement a valid sequence at 1.5T
- Describe the incidence of perivenular lesions at 1.5T in a small population of clinically diagnosed MS patients.

Methods

FLAIR* at 7T versus FLAIR* at 3T

In this pilot study, nine patients with a clinically definite diagnosis of MS in accordance with the 2010 revised McDonald criteria⁷ were selected from our database. Demographic and clinical data are showed in following table.

Demographic data:

| | Sex | Age (years) | Diagnosis | Disease duration (years) | Time between scans (months) |
|------|-----|-------------|-----------|--------------------------|-----------------------------|
| Pt 1 | F | 58 | RR-MS | 10.3 | 7.8 |
| Pt 2 | F | 33 | RR-MS | 0.9 | 12 |
| Pt 3 | F | 30 | RR-MS | 4.7 | 13 |
| Pt 4 | F | 38 | RR-MS | 7.9 | 11 |
| Pt 5 | F | 39 | RR-MS | 7.4 | 18 |
| Pt 5 | F | 28 | RR-MS | 0.8 | 12 |
| Pt 6 | M | 32 | RR-MS | 4.1 | 10 |
| Pt 7 | F | 49 | RR-MS | 19 | 12 |
| Pt 8 | F | 44 | RR-MS | 1.7 | 12 |

Patients gave written informed consent in accordance with the institutional review board. All patients underwent to a clinical scan with a Siemens 3 T Skyra system and a 32-channel phased-array receive-only head coil. T2-FLAIR and T2 * EPI were acquired. T2*-EPI was also repeated approximately 4 minutes after 0.1 mmol of gadolinium injection. Detailed parameters are provided in table below. These three dimensional sequences were acquired in the sagittal plane, covering the full brain. Additional sequences were also acquired for clinical purposes.

The same patients underwent to a 7 T MRI Siemen. Scan included a three dimensional T2-FLAIR and a three dimensional T2* EPI. Detailed parameters are provided in the following table.

MRI sequences parameters:

| | 3 T sequences | | 7 T sequences | |
|------------------------|---------------|----------------|---------------|-------------|
| | T2-FLAIR | T2*-EPI | T2-FLAIR | T2*-EPI |
| Repetition time (msec) | 4800 | 64 | 8000 | 52 |
| Echo time (msec) | 354 | 35 | 399 | 23 |
| Inversion time (msec) | 1800 | - | 2150 | - |
| Flip angle (°) | 120° | 10° | 120° | 10° |
| Field of view | 256x256 | 384x312 | 320x280 | 180x280 |
| Voxel resolution | 1x1x1 | 0.65x0.65x0.65 | 0.8x0.8x0.8 | 0.5x0.5x0.5 |
| Acquisition time | 5:12 | 5:44 | 6:26 | 3:40 |

Additional sequences were acquired.

Mean time between the two scans was 11 months (range: 8-18 months).

Image processing

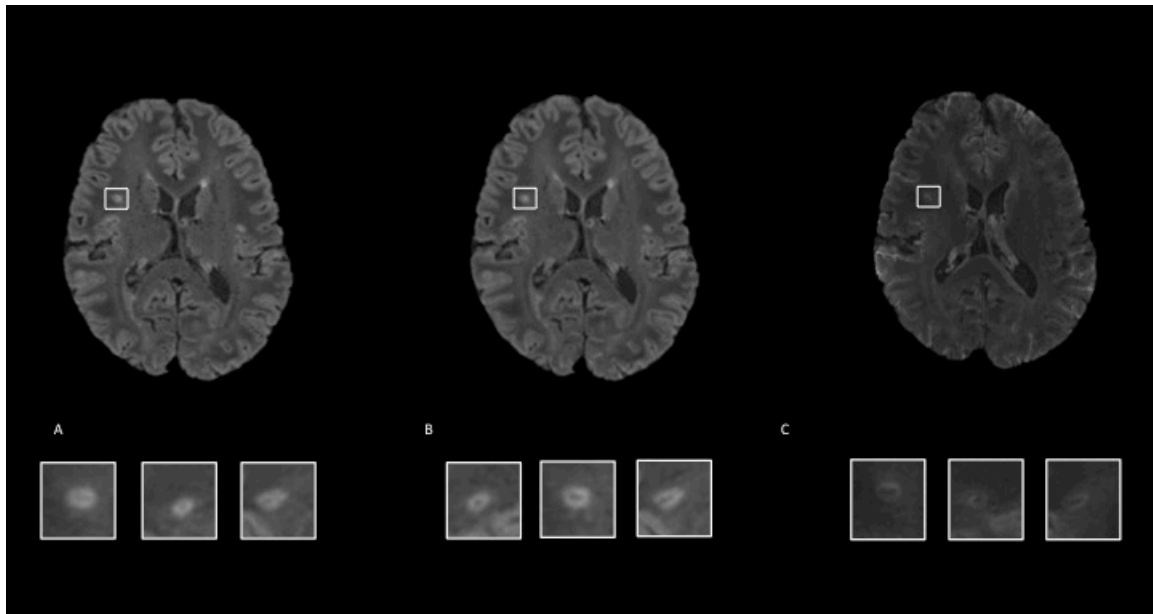
3T pre-gad FLAIR*, 3T post-gad FLAIR* were obtained processing T2-FLAIR and T2* EPI respectively pre and post gad by an expert operator, using a pipeline in MIPAV (Medical Image Processing, Analysis & Visualization, National Institutes of Health; mipav.cit.nih.gov), as previously describe ⁸¹. 7T FLAIR* also were processing according previously described ⁹³.

3T FLAIR* and 7T FLAIR* were evaluated by an expert observer (nine years of experience in MS imaging), blinded to clinical data, on a dedicate console using MIPAV software.

Total number of lesions (L) was reported. Lesions were considered perivenular (VL) if the presence of hypointense signal was noted in at least 2 perpendicular plans and if it was completely surrounded by hyperintense signal in at least 1 plane.

At a later stage, 3T post-gd FLAIR* and 7T FLAIR* were registered on the 3T pre-gd FLAIR* in order to directly compare each lesion. Only lesions visible on all the scans were considered in the analysis.

Chi-square test was used to compare number of VL between scans.



FLAIR* at 7T versus FLAIR* at 3T: Axial 3T pre-gd FLAIR* (A), 3T post-gd FLAIR* (B) and a 7T FLAIR* (C) in a 44-year-old woman with relapsing-remitting MS (EDSS= 6.5, disease duration=1.7y) show a lesion in in the right frontal white matter. Although better appreciable on the 3T post-gd FLAIR* and on 7T FLAIR*, the vein inside the lesion is visible on all the three sequences. In the latter row, the same lesion

from each sequence is magnified and showed on the three orthogonal planes (respectively axial, sagittal and coronal).

Study at 1.5T

A SWI at high resolution was implemented at 1.5T (Philips, Achieva), head coil 8ch.

The following MRI protocol was used:

- MPRAGE
- Gadolinium administration (0.1 mmol/kg)
- SWI
- MPRAGE
- 3-D FLAIR

Detailed MRI sequence parameters are described in the table below:

| | 1.5 T sequences | |
|------------------------|-----------------|----------------|
| | T2-FLAIR | SWI |
| Repetition time (msec) | 4800 | 44 |
| Echo time (msec) | 357 | 23 |
| Inversion time (msec) | 1660 | - |
| Flip angle (°) | 90° | 10° |
| Field of view | 256x256x1802 | 240x240x176 |
| Voxel resolution | 1x1x1 | 0.53x0.53x0.53 |
| Acquisition time | 4:30 | 8:17 |

The gad was administered using a power injector at a slow flow (0.34 ml/min)

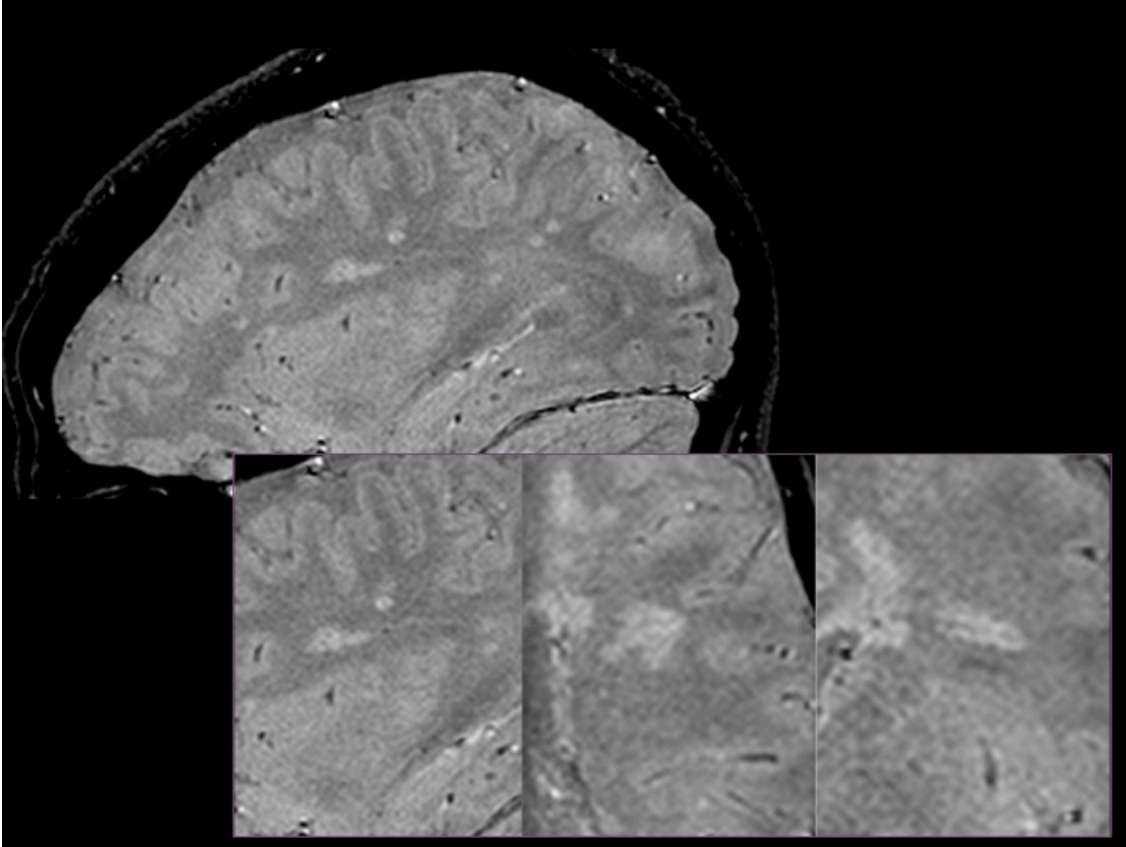
Ten patients with a clinically definite diagnosis of MS in accordance with the 2010 revised McDonald criteria⁷ were selected randomly from our database. Demographic and clinical data are showed in following table.

| | Sex | Age (years) | Diagnosis | Disease duration (years) |
|------|-----|-------------|-----------|--------------------------|
| Pt 1 | F | 20 | RR-MS | 2 |
| Pt 2 | F | 47 | RR-MS | 23 |
| Pt 3 | F | 52 | RR-MS | 14 |
| Pt 4 | F | 54 | RR-MS | 7 |
| Pt 5 | F | 35 | RR-MS | 13 |
| Pt 6 | M | 61 | RR-MS | 18 |
| Pt 7 | F | 36 | RR-MS | |
| Pt 8 | F | 23 | RR-MS | 9 |
| Pt9 | F | 51 | RR-MS | 12 |
| Pt10 | F | 34 | RR-MS | 5 |

SWI and FLAIR images were evaluated by an expert observer (nine years of experience in MS imaging), blinded to clinical data, on a console using OsiriX software.

The total number of lesions was analyzed in the FLAIR scans, whereas the venules and their relations with the lesions, in the SWI scan coregistrated to the FLAIR scans.

Total number of lesions (L) was reported from FLAIR. Each lesion was found back on the SWI in order analyze their relationship with the vein. Lesions were considered perivenular (VL) if the presence of hypointense signal was noted in at least 2 perpendicular plans and if it was completely surrounded by hyperintense signal in at least 1 plane.



SWI at 1.5T: *A 20-year-old Relapsing-Remitting Multiple Sclerosis (EDSS= 1; disease duration= 2 years) presents different lesions with typical perivenular distribution.*

In the second line, the same lesions are shown in the three different planes (sagittal, axial, coronal).

Results

Comparison of FLAIR* at 3T and 7T

In total, 411 lesions were considered in the analysis. Mean number of lesions per patient was 45 (± 25).

When compared the three sub-sets of images, 310 lesions were clearly visible on all the images and therefore considered for the analysis. Mean number of lesions per patients was 38 (± 28).

7T FLAIR* was more sensitive in detecting the VL than the 3T pre-gad FLAIR* ($p=0.02$) and the 3T post-gd FLAIR* ($p=0.02$). The administration of gad increased the number of VL ($p=0.04$). The number of NVL is shown in table below.

| | 3T pre-gad FLAIR* | | | 3T post-gd FLAIR* | | | 7T FLAIR* | | |
|------------|-------------------|-----|--------|-------------------|-----|--------|-----------|-----|--------|
| | VL | NVL | % vein | VL | NVL | % vein | VL | NVL | % vein |
| Pt1 | 32 | 3 | 91 | 33 | 2 | 94 | 35 | 0 | 100 |
| Pt2 | 31 | 9 | 78 | 32 | 8 | 80 | 39 | 1 | 98 |
| Pt3 | 56 | 4 | 93 | 57 | 3 | 95 | 58 | 2 | 97 |
| Pt4 | 47 | 6 | 89 | 47 | 6 | 89 | 50 | 3 | 94 |
| Pt5 | 39 | 2 | 95 | 39 | 2 | 95 | 40 | 1 | 98 |
| Pt6 | 11 | 0 | 100 | 11 | 0 | 100 | 11 | 0 | 100 |
| Pt7 | 13 | 4 | 76 | 15 | 2 | 88 | 17 | 0 | 100 |
| Pt8 | 60 | 0 | 100 | 60 | 0 | 100 | 60 | 0 | 100 |
| Pt9 | 85 | 9 | 90 | 86 | 8 | 91 | 91 | 3 | 97 |

| | | | | | | | | | |
|----------------|---------|-------|----------|---------|-------|----------|---------|-------|----------|
| Mean | 42 | 4 | 90 | 42 | 3 | 93 | 45 | 1 | 98 |
| Median | 35 | 3.5 | 92 | 36 | 2 | 94.5 | 39 | 0.5 | 99 |
| (Range) | (11-85) | (0-9) | (76-100) | (11-86) | (0-8) | (80-100) | (11-91) | (0-3) | (94-100) |

Abbr. VL: vein lesion; NVL: lesion without vein

Results at 1.5 T

In total, 284 lesions were considered in the analysis. All the lesions were considered in the analysis. Mean number of lesions per patient was 28 (± 14).

The mean percentage of lesions with a vein was 81% ($\pm 11\%$)

Detailed analysis is shown in the following table.

| | VL | NVL | L | % |
|----------------|-----------|-----------|--------------|------------|
| Pt1 | 7 | 4 | 11 | 63 |
| Pt2 | 24 | 2 | 26 | 92 |
| Pt3 | 44 | 5 | 49 | 89 |
| Pt4 | 32 | 5 | 37 | 86 |
| Pt5 | 7 | 3 | 10 | 70 |
| Pt6 | 39 | 2 | 41 | 95 |
| Pt7 | 13 | 4 | 17 | 76 |
| Pt8 | 24 | 5 | 29 | 82 |
| Pt9 | 40 | 5 | 45 | 88 |
| Pt10 | 13 | 6 | 19 | 68 |
| Mean | 24 | 4 | 28 | 81 |
| Median (range) | 24 (7-44) | 4.5 (2-6) | 27.5 (10-49) | 84 (63-95) |

Discussion

In this study, we explored the relationship between MS lesions and a central vein at different magnetic fields (1.5T, 3T and 7T).

As Charcot described in 1868⁷⁶ and later Dawson⁷⁷ in 1916, a small vein centers the MS plaque. Many studies suggest that the pathogenic processes involved in the onset and enlargement of MS plaques start from lympho-monocytic infiltrates surrounding the one vein⁹⁴.

We implemented a FLAIR* on ultra-high magnetic field (7T) and we acquired the same patients at 3T and 7T, thus being able to evaluate exactly the same lesions.

Our 7T-FLAIR* showed that virtually all MS lesions, even the smaller were centered on a central vein, these results are in line with the pathological finding⁷⁶.

Indeed, also 3T FLAIR* showed a remarkably high percentage of perivenular lesions. All the lesions centered on a vein on 3T were also perivenular on 7T, confirming that 7T was more sensitive than 3T and not controversial.

The contrast administration increased the efficiency, even not dramatically.

Contrast administration is mandatory in a diagnostic workup, otherwise if it is not clinically required a FLAIR* without contrast could be sufficient to demonstrate the perivenular distribution of MS lesions.

Furthermore, we set-up a high resolution SWI sequence on a 1.5T. Unfortunately, we were not able to acquire the same patients on this magnetic field and thus to perform a direct comparison. However we selected a representative group of patients and we could speculate about the sensibility of the 1.5T, comparing the median percentage.

Impressively, just one first study⁸³ described the percentage of perivenular lesions in MS at a low magnetic field, despite the 1.5T is still the most diffuse magnetic field strength in the clinical practice.

In our population the median percentage of lesions was 84%. The lowest percentage was 63%.

Thus, even with the aforementioned limitation, we can affirm that 1.5T sensitivity was lower than the 3T.

Remarkably, our finding was profusely higher than the cut-off of 45% proposed by Tallantyre⁸⁵ to discriminate MS lesions from other pathological conditions.

Nevertheless, this study is limited by the small number of patients observed that could not be representative of the overall population.

A wider number of patients is required to better characterize MS population and to set a cut-off limit suggestive for MS or not.

Despite these limitations, our study confirms that the evaluation of MS lesions perivenular distribution is feasible also in a clinical setting at a lower magnetic field.

Since this feature, previously described in histopathology is strongly suggestive of a demyelination process, we can propose this marker as indicative of MS.

Although further studies are required to determine the applicability in the differential diagnosis of white matter lesions, these data are really promising.

Conclusions

Multiple Sclerosis is characterized by a great variability and clinical outcome is largely unpredictable for individual patients. This complexity highlights the need for reliable biological markers with high sensitivity and specificity that are able to help in the diagnosis and predict the future disease course and the treatment response.

Unfortunately peripheral disease markers are inappropriate, since Central Nervous System presents an isolated environment.

The only opportunity to study the disease in vivo is CSF sampling and MR imaging. In particular, MR imaging allow us to longitudinally study patients without any risks.

Thanks to advanced techniques, we are able to explore histopathological knowledge and apply it to in vivo studies.

In the first part, we described the prevalence and clinical correlation of leptomeningeal enhancement and we proposed it as the first in vivo marker of leptomeningeal inflammation. Our hypothesis was supported by two pathological reports. Despite the aforementioned limitations, the possibility to study the meningeal inflammation in vivo is charming. First of all, it could be used to better stratify patients on the basis of the presence of leptomeningeal inflammation in order to detect a subgroup that could be address to a more specific intrathecal therapy. Furthermore, this marker could be used to monitor the response to specific drugs.

In the second study, we documented in vivo the association between Multiple Sclerosis lesions and a central vein. The comparison at different magnetic fields demonstrated that also low magnetic field could be efficient allowing the utilization of this marker in a

clinical setting. The utility in the differential diagnosis is promising, although further studies are required to support this hypothesis.

In both of these two studies, a hypothesis arising from well-known histopathological MS features (leptomeningeal inflammation and lesion/vein association) has been confirmed in vivo on the basis of MR Imaging.

Ultra-high field MRI proved to be helpful in documenting the corresponding findings in a research setting, thus establishing a link between pathology and clinical research. Thanks to the advantages deriving from it, we are able to translate our expertise to a lower magnetic field in order to apply them to wider scale.

Even considering the lower sensitivity, 1.5T routine MRI appears to be effective and widely applicable, on regard of both of the two described features.

References

1. Weinshenker, b. G. *Et al.* The natural history of multiple sclerosis: a geographically based study. *Brain* **112**, 1419–1428 (1989).
2. Koch-Henriksen, N. & Sørensen, P. S. The changing demographic pattern of multiple sclerosis epidemiology. *The Lancet Neurology* **9**, 520–532 (2010).
3. Ebers, G. C. Environmental factors and multiple sclerosis. *Lancet Neurol.* **7**, 268–277 (2008).
4. Lublin, F. D. & Reingold, S. C. Defining the clinical course of multiple sclerosis: results of an international survey. National Multiple Sclerosis Society (USA) Advisory Committee on Clinical Trials of New Agents in Multiple Sclerosis. *Neurology* **46**, 907–911 (1996).
5. Ramsaransing, G. S. M. & De Keyser, J. Benign course in multiple sclerosis: A review. *Acta Neurologica Scandinavica* **113**, 359–369 (2006).
6. Scalfari, A. *et al.* The natural history of multiple sclerosis, a geographically based study 10: Relapses and long-term disability. *Brain* **133**, 1914–1929 (2010).
7. Polman, C. H. *et al.* Diagnostic criteria for multiple sclerosis: 2010 Revisions to the McDonald criteria. *Ann. Neurol.* **69**, 292–302 (2011).
8. Greenfield, E. A. *et al.* Monoclonal antibodies to distinct regions of human myelin proteolipid protein simultaneously recognize central nervous system myelin and neurons of many vertebrate species. *J. Neurosci. Res.* **83**, 415–431 (2006).
9. De Stefano, N. *et al.* Evidence of early cortical atrophy in MS: relevance to white matter changes and disability. *Neurology* **60**, 1157–1162 (2003).
10. Calabrese, M. *et al.* No MRI evidence of cortical lesions in neuromyelitis optica. *Neurology* **79**, 1671–1676 (2012).
11. Absinta, M. *et al.* Patients with migraine do not have MRI-visible cortical lesions. *J. Neurol.* **259**, 2695–2698 (2012).
12. Peterson, J. W., Bö, L., Mörk, S., Chang, A. & Trapp, B. D. Transected neurites, apoptotic neurons, and reduced inflammation in cortical multiple sclerosis lesions. *Ann. Neurol.* **50**, 389–400 (2001).

13. Lucchinetti, C. F. *et al.* Inflammatory Cortical Demyelination in Early Multiple Sclerosis. *New England Journal of Medicine* **365**, 2188–2197 (2011).
14. Lassmann, H., Brück, W. & Lucchinetti, C. F. The immunopathology of multiple sclerosis: An overview. in *Brain Pathology* **17**, 210–218 (2007).
15. Lövblad, K.-O. *et al.* MR imaging in multiple sclerosis: review and recommendations for current practice. *AJNR. Am. J. Neuroradiol.* **31**, 983–989 (2010).
16. Filippi, M. & Rocca, M. A. MR imaging of multiple sclerosis. *Radiology* **259**, 659–681 (2011).
17. Li, D. K. B. *et al.* MRI T2 lesion burden in multiple sclerosis: A plateauing relationship with clinical disability. *Neurology* **66**, 1384–1389 (2006).
18. Sormani, M. P. *et al.* Magnetic resonance imaging as a potential surrogate for relapses in multiple sclerosis: A meta-analytic approach. *Ann. Neurol.* **65**, 268–275 (2009).
19. Sormani, M. P. *et al.* Surrogate endpoints for EDSS worsening in multiple sclerosis: A meta-analytic approach. *Neurology* **75**, 302–309 (2010).
20. Cotton, F., Weiner, H. L., Jolesz, F. A. & Guttmann, C. R. G. *MRI contrast uptake in new lesions in relapsing-remitting MS followed at weekly intervals.* *Neurology* **60**, 640–646 (2003).
21. Gaitán, M. I. *et al.* Evolution of the blood-brain barrier in newly forming multiple sclerosis lesions. *Ann. Neurol.* **70**, 22–29 (2011).
22. Schwartz, K. M., Erickson, B. J. & Lucchinetti, C. Pattern of T2 hypointensity associated with ring-enhancing brain lesions can help to differentiate pathology. *Neuroradiology* **48**, 143–149 (2006).
23. Maggi, P. *et al.* The formation of inflammatory demyelinated lesions in cerebral white matter. *Ann. Neurol.* **76**, 594–608 (2014).
24. Wiggermann, V. *et al.* Magnetic resonance frequency shifts during acute MS lesion formation. *Neurology* **81**, 211–218 (2013).
25. Moll, N. M. *et al.* Multiple sclerosis normal-appearing white matter: Pathology-imaging correlations. *Ann. Neurol.* **70**, 764–773 (2011).
26. Cercignani, M., Bozzali, M., Iannucci, G., Comi, G. & Filippi, M. Magnetisation transfer ratio and mean diffusivity of normal appearing white and grey matter from

- patients with multiple sclerosis. *J. Neurol. Neurosurg. Psychiatry* **70**, 311–317 (2001).
27. De Stefano, N., Battaglini, M. & Smith, S. M. Measuring brain atrophy in multiple sclerosis. *J. Neuroimaging* **17**, (2007).
 28. Liu, W., Nair, G., Vuolo, L. & Bakshi, A. In vivo imaging of spinal cord atrophy in neuroinflammatory diseases. *Ann. ...* **76**, 370–8 (2014).
 29. Lycklama À Nijeholt, G. J. Reduction of brain volume in MS. MRI and pathology findings. in *Journal of the Neurological Sciences* **233**, 199–202 (2005).
 30. Giorgio, A. & De Stefano, N. Clinical use of brain volumetry. *Journal of Magnetic Resonance Imaging* **37**, 1–14 (2013).
 31. Kidd, D. Cortical lesions in multiple sclerosis. *Brain* **122**, 17–26 (1999).
 32. Geurts, J. J. & Barkhof, F. Grey matter pathology in multiple sclerosis. *The Lancet Neurology* **7**, 841–851 (2008).
 33. Van Horsen, J., Brink, B. P., de Vries, H. E., van der Valk, P. & Bø, L. The blood-brain barrier in cortical multiple sclerosis lesions. *J. Neuropathol. Exp. Neurol.* **66**, 321–328 (2007).
 34. Hulst, H. E. & Geurts, J. J. G. Gray matter imaging in multiple sclerosis: what have we learned? *BMC Neurol.* **11**, 153 (2011).
 35. Schmierer, K. *et al.* High field (9.4 Tesla) magnetic resonance imaging of cortical grey matter lesions in multiple sclerosis. *Brain* **133**, 858–867 (2010).
 36. Geurts, J. J. G. *et al.* Intracortical lesions in multiple sclerosis: improved detection with 3D double inversion-recovery MR imaging. *Radiology* **236**, 254–260 (2005).
 37. Nelson, F., Poonawalla, A., Hou, P., Wolinsky, J. S. & Narayana, P. A. *3D MPRAGE improves classification of cortical lesions in multiple sclerosis. Multiple sclerosis (Houndmills, Basingstoke, England)* **14**, 1214–1219 (2008).
 38. Kilsdonk, I. D. *et al.* Multicontrast MR imaging at 7T in multiple sclerosis: Highest lesion detection in cortical gray matter with 3D-FLAIR. *Am. J. Neuroradiol.* **34**, 791–796 (2013).
 39. Nielsen, A. S. *et al.* Focal cortical lesion detection in multiple sclerosis: 3 tesla DIR versus 7 tesla FLASH-T2. *J. Magn. Reson. Imaging* **35**, 537–542 (2012).
 40. Geurts, J. J. G. *et al.* Consensus recommendations for MS cortical lesion scoring using double inversion recovery MRI. *Neurology* **76**, 418–424 (2011).

41. Ikuta, F. & Zimmerman, H. M. Distribution of plaques in seventy autopsy cases of multiple sclerosis in the United States. *Neurology* **26**, 26–28 (1976).
42. Hittmair, K., Mallek, R., Prayer, D., Schindler, E. G. & Kollegger, H. Spinal cord lesions in patients with multiple sclerosis: comparison of MR pulse sequences. *AJNR. Am. J. Neuroradiol.* **17**, 1555–1565 (1996).
43. Nair, G., Absinta, M. & Reich, D. S. Optimized T1-MPRAGE sequence for better visualization of spinal cord multiple sclerosis lesions at 3T. *Am. J. Neuroradiol.* **34**, 2215–2222 (2013).
44. Martin, N. *et al.* Comparison of MERGE and axial T2-weighted fast spin-echo sequences for detection of multiple sclerosis lesions in the cervical spinal cord. *Am. J. Roentgenol.* **199**, 157–162 (2012).
45. Lycklama, G. *et al.* Spinal-cord MRI in multiple sclerosis. *Lancet Neurology* **2**, 555–562 (2003).
46. Hickman, S. J. Optic nerve imaging in multiple sclerosis. *J. Neuroimaging* **17 Suppl 1**, 42S–45S (2007).
47. Hodel, J. *et al.* Comparison of 3D double inversion recovery and 2D STIR FLAIR MR sequences for the imaging of optic neuritis: pilot study. (2014). doi:10.1007/s00330-014-3342-3
48. Mistry, N. *et al.* Focal multiple sclerosis lesions abound in “normal appearing white matter.” *Multiple Sclerosis Journal* **17**, 1313–1323 (2011).
49. Kilsdonk, I. D. *et al.* Morphological features of MS lesions on FLAIR at 7 T and their relation to patient characteristics. *J. Neurol.* **261**, 1356–1364 (2014).
50. Absinta, M. *et al.* Seven-tesla phase imaging of acute multiple sclerosis lesions: A new window into the inflammatory process. *Ann. Neurol.* **74**, 669–678 (2013).
51. Mainero, C. *et al.* In vivo imaging of cortical pathology in multiple sclerosis using ultra-high field MRI. *Neurology* **73**, 941–948 (2009).
52. Absinta, M. *et al.* Postmortem magnetic resonance imaging to guide the pathologic cut: individualized, 3-dimensionally printed cutting boxes for fixed brains. *J. Neuropathol. Exp. Neurol.* **73**, 780–8 (2014).
53. Decimo, I., Fumagalli, G., Berton, V., Krampera, M. & Bifari, F. Meninges: from protective membrane to stem cell niche. *Am. J. Stem Cells* **1**, 92–105 (2012).
54. Choi, S. R. *et al.* Meningeal inflammation plays a role in the pathology of primary progressive multiple sclerosis. *Brain* **135**, 2925–2937 (2012).

55. Magliozzi, R. *et al.* A Gradient of neuronal loss and meningeal inflammation in multiple sclerosis. *Ann. Neurol.* **68**, 477–493 (2010).
56. Magliozzi, R. *et al.* Meningeal B-cell follicles in secondary progressive multiple sclerosis associate with early onset of disease and severe cortical pathology. *Brain* **130**, 1089–1104 (2007).
57. Serafini, B., Rosicarelli, B., Magliozzi, R., Stigliano, E. & Aloisi, F. Detection of ectopic B-cell follicles with germinal centers in the meninges of patients with secondary progressive multiple sclerosis. *Brain Pathol.* **14**, 164–174 (2004).
58. Howell, O. W. *et al.* Meningeal inflammation is widespread and linked to cortical pathology in multiple sclerosis. *Brain* **134**, 2755–2771 (2011).
59. Serafini, B. *et al.* Dysregulated Epstein-Barr virus infection in the multiple sclerosis brain. *J. Exp. Med.* **204**, 2899–2912 (2007).
60. Bradley WG, S. D. *Magnetic resonance imaging.* (1999). doi:0815185189
61. Charil, A. *et al.* MRI and the diagnosis of multiple sclerosis: expanding the concept of “no better explanation.” *Lancet Neurology* **5**, 841–852 (2006).
62. Miller, D. H. *et al.* Differential diagnosis of suspected multiple sclerosis: a consensus approach. in *Multiple sclerosis (Houndmills, Basingstoke, England)* **14**, 1157–1174 (2008).
63. Demaerel, P. H. *et al.* Focal Leptomeningeal MR Enhancement along the Chiasm as a Presenting Sign of Multiple Sclerosis. *Journal of Computer Assisted Tomography* **19**, 297–298 (1995).
64. F Barkhof, J Valk, O R Hommes, and P. S. meningeal gd-DPTA enhancement in multiple sclerosis. *AJNR. Am. J. Neuroradiol.* (1992).
65. Mamourian, A. C., Jack Hoopes, P. & Lewis, L. D. Visualization of Intravenously Administered Contrast Material in the CSF on Fluid-Attenuated Inversion-Recovery MR Images: An In Vitro and Animal-Model Investigation. *AJNR Am. J. Neuroradiol.* **21**, 105–111 (2000).
66. Kataoka, H., Taoka, T. & Ueno, S. Early contrast-enhanced magnetic resonance imaging with fluid-attenuated inversion recovery in multiple sclerosis. *J Neuroimaging* **19**, 246–249 (2009).
67. Shiee, N. *et al.* A topology-preserving approach to the segmentation of brain images with multiple sclerosis lesions. *Neuroimage* **49**, 1524–1535 (2010).

68. Kramer, L. A. *et al.* Contrast enhanced MR venography with gadofosveset trisodium: Evaluation of the intracranial and extracranial venous system. *J. Magn. Reson. Imaging* **40**, 630–640 (2014).
69. Kremer, S. *et al.* Evaluation of an albumin-binding gadolinium contrast agent in multiple sclerosis. *Neurology* **81**, 206–210 (2013).
70. Mancardi, G. *et al.* Autologous haematopoietic stem cell transplantation with an intermediate intensity conditioning regimen in multiple sclerosis: the Italian multi-centre experience. *Multiple Sclerosis Journal* **18**, 835–842 (2012).
71. Roccatagliata, L. *et al.* The long-term effect of AHSC on MRI measures of MS evolution: a five-year follow-up study. *Multiple sclerosis (Houndmills, Basingstoke, England)* **13**, 1068–1070 (2007).
72. Marjanovic, Z., Snowden, J., Badoglio, M., Saccardi, R. & Farge, D. Long-term outcomes of autologous haematopoietic stem cell transplantation in severe autoimmune diseases: An extended analysis of the EBMT database 1996-2011. *Bone Marrow Transplant.* **47**, S224–S224 (2012).
73. Mancardi, G. *et al.* Autologous haematopoietic stem cell transplantation in Multiple Sclerosis (ASTIMS): a phase II, randomized, active-controlled, multicenter trial. *Neurology in press*, (2015).
74. Bowen, J. D. *et al.* Autologous hematopoietic cell transplantation following high-dose immunosuppressive therapy for advanced multiple sclerosis: long-term results. *Bone Marrow Transplantation* **47**, 946–951 (2012).
75. Muraro, P. A. *et al.* Thymic output generates a new and diverse TCR repertoire after autologous stem cell transplantation in multiple sclerosis patients. *The Journal of experimental medicine* **201**, 805–816 (2005).
76. Fog, T. The topography of plaques in multiple sclerosis with special reference to cerebral plaques. *Acta Neurol. Scand. Suppl.* (1964). at <<http://europepmc.org/abstract/MED/5213727>>
77. Dawson, J. W. XVIII The Histology of Disseminated Sclerosis. *Earth Environ. Sci. Trans. R. Soc. Edinburgh* **50**, 517–740 (1916).
78. Agrawal, S. M. *et al.* Extracellular matrix metalloproteinase inducer shows active perivascular cuffs in multiple sclerosis. *Brain* **136**, 1760–1777 (2013).
79. Haacke, E. M., Xu, Y., Cheng, Y.-C. N. & Reichenbach, J. R. Susceptibility weighted imaging (SWI). *Magn. Reson. Med.* **52**, 612–618 (2004).

80. Grabner, G. *et al.* Analysis of multiple sclerosis lesions using a fusion of 3.0 T FLAIR and 7.0 T SWI phase: FLAIR SWI. *J. Magn. Reson. Imaging* **33**, 543–549 (2011).
81. Sati, P., George, I. C., Shea, C. D., Gaitan, M. I. & Reich, D. S. FLAIR*: A Combined MR Contrast Technique for Visualizing White Matter Lesions and Parenchymal Veins. *Radiology* (2012). doi:10.1148/radiol.12120208
82. Kilsdonk, I. D. *et al.* Improved differentiation between MS and vascular brain lesions using FLAIR* at 7 Tesla. *Eur. Radiol.* **24**, 841–849 (2014).
83. Tan, I. L. *et al.* MR venography of multiple sclerosis. *Am. J. Neuroradiol.* **21**, 1039–1042 (2000).
84. Ge, Y., Zohrabian, V. M. & Grossman, R. I. *Seven-Tesla magnetic resonance imaging: new vision of microvascular abnormalities in multiple sclerosis.* *Archives of neurology* **65**, 812–816 (2008).
85. Tallantyre, E. C. *et al.* Demonstrating the perivascular distribution of MS lesions in vivo with 7-Tesla MRI. *Neurology* **70**, 2076–8 (2008).
86. Tallantyre, E. C. *et al.* A comparison of 3T and 7T in the detection of small parenchymal veins within MS lesions. *Investigative radiology* **44**, 491–4 (2009).
87. Lummel, N. *et al.* Presence of a central vein within white matter lesions on susceptibility weighted imaging: A specific finding for multiple sclerosis? *Neuroradiology* **53**, 311–317 (2011).
88. Mistry, N. *et al.* 3T T2* Mri Distinguishes Ms From Microangiopathic Lesions. *Journal of Neurology, Neurosurgery & Psychiatry* **85**, e4–e4 (2014).
89. Wuerfel, J. *et al.* Lesion morphology at 7 Tesla MRI differentiates Susac syndrome from multiple sclerosis. *Multiple Sclerosis Journal* **18**, 1592–1599 (2012).
90. Sinnecker, T. *et al.* Distinct lesion morphology at 7-T MRI differentiates neuromyelitis optica from multiple sclerosis. *Neurology* **79**, 708–714 (2012).
91. Kau, T. *et al.* The “central vein sign”: Is there a place for susceptibility weighted imaging in possible multiple sclerosis? *Eur. Radiol.* **23**, 1956–1962 (2013).
92. Mistry, N. *et al.* Central veins in brain lesions visualized with high-field magnetic resonance imaging: a pathologically specific diagnostic biomarker for inflammatory demyelination in the brain. *JAMA Neurol.* **70**, 623–8 (2013).

93. Dewey BE, Sati P, Vuolo L, Shea C, Inati D, R. D. 7T FLAIR_ Acquisition and Processing- Application to Multiple Sclerosis. in (2014).
94. Adams, C. W. M. The onset and progression of the lesion in multiple sclerosis. *J. Neurol. Sci.* **25**, 165–182 (1975).